SMARTPHONE-BASED SYSTEMS FOR MOBILE INFECTIOUS DISEASE DETECTION AND EPIDEMIOLOGY

BY

WEILI CHEN

DISSERTATION

Submitted in partial fulfillment of the requirements
for the degree of Doctor of Philosophy in Electrical and Computer Engineering
in the Graduate College of the
University of Illinois at Urbana-Champaign, 2017

Urbana, Illinois

Doctoral Committee:

Professor Brian T. Cunningham, Chair
Professor Rashid Bashir
Professor J. Gary Eden
Research Scientist Ian Brooks

ABSTRACT

Infectious diseases remain a serious public health challenge worldwide and are the leading cause of death in many developing countries. The rapid detection of pathogens is vital for the control and prevention of the infectious diseases. New tools are needed to enable rapid detection, identification, and reporting of infectious viral and microbial pathogens in a wide variety of point-of-care applications that impact human and animal health. With the rapid development of mobile technologies, mobile devices have provided a novel and effective approach to identify and report infectious diseases.

In this work, two types of smartphone-based detection platforms are developed for mobile infectious disease detection. The first one is for the detection of human immunodeficiency virus. The second one is for the multiplexed detection of nucleic acids of pathogens for equine respiratory infections. Both platforms utilize a smartphone camera as the sensor in conjunction with a handheld cradle that interfaces the phone with a microchip for the on-chip nucleic acid testing of infectious diseases.

This work provides a mobile, simple and inexpensive capability for clinicians to perform infectious disease diagnostics, and it represents a significant stride towards a practical solution to the infectious disease diagnostics at resource-limited settings.

ACKNOWLEDGMENTS

First of all, I would like to thank my advisor Professor Brian T. Cunningham for giving me the opportunity to work in one of the best engineering schools in the world. Without his valuable guidance and firm support, it would be impossible for me to overcome all the difficulties in this research project and write this dissertation to sum up my research results obtained in the last two years.

I also wish to acknowledge several past and present members of the Nano Sensors Research Group: Dr. Meng Lu, Dr. Vikram Chaudhery, Dr. Erich Lidstone, Dr. Anusha Pokhriyal, Dr. Meng Zhang, Dr. Yafang Tan, Dr. Jui-Nung Liu, Dr. Gloria See, Kenny Long and Hojeong Yu. The experience and knowledge selflessly shared by them laid a strong foundation for any achievement that I could accomplish. Also, I am thankful for on-campus collaborators including Dr. Gregory Damhorst, Akid Ornob, Professor Rashid Bashir and, Professor Ian Brooks, as well as off-campus collaborators including Professor David Hirschberg from University of Washington and Dr. David Nash from Kentucky.

I am deeply grateful for my parents. The spirit of enterprise, responsibility, kindness and firmness I learned from them are the rocks of my life. Their encouragement makes me feel fearless for the future and they are always in my heart.

Thanks for both the good times and hard times.

TABLE OF CONTENTS

LIST OF ABBREVIATIONS

3D	three-dimensional
AIDS	acquired immune deficiency syndrome
DNA	deoxyribonucleic acid
EHV	equine herpesvirus
EVD	ebola virus disease
HIV	human immunodeficiency virus
LAMP	loop mediated isothermal amplification
LED	light-emitting diode
LOP	lab-on-a-chip
MEMS	micro-electro-mechanical-system
mHealth	mobile health
NAT	nucleic acid testing
PCR	polymerase chain reaction
POC	point-of-care
QR	quick response
RT	reverse transcription
SARS	severe acute respiratory syndrome
WHO	world health organization

CHAPTER 1

INTRODUCTION

1.1 Infectious disease

Historically, infectious diseases have hugely impacted humankind as one of the most important contributors to human morbidity and mortality [1]. Today, such diseases remain a serious public health threat. Despite the significant accomplishments made in the diagnosis, prevention and treatment of infectious diseases during the 20th century [2], the outbreaks of new infectious diseases such as HIV/AIDS, severe acute respiratory syndrome (SARS), Ebola virus disease (EVD), and Zika virus disease have significantly increased during the past two decades [3]. The re-emergence of diseases previously regarded as under control such as malaria and cholera has also drawn considerable attention [4]. According to the world health report released by the World Health Organization (WHO) in 2004, infectious diseases are responsible for approximately 25.9% of global deaths, with the leading causes being lower-respiratory infections (6.9%), HIV/AIDS (4.9%), diarrhea (3.2%) and tuberculosis (TB) (2.7%) [5]. While infectious diseases are not prevalent in the developed countries, large parts of developing countries, especially sub-Saharan African countries, are still vulnerable to such diseases due to the insufficient medical resources and effective public health surveillance system, and therefore account for more than half of infectious disease deaths [6]. On the other hand, with the rapid population

mobility brought by globalization, the differences in infectious disease epidemiology are reduced among different regions of the world [7]. Local epidemics can quickly become regional or even global issues.

Infectious diseases can also destructively affect animals and plants. The incidence of infectious diseases among animals and plants can pose a serious threat to food safety, environment protection and national economies. For example, the outbreaks of Avian influenza between 1996 and 2008, which is commonly known as the "bird flu" because of the viruses adapted to birds, spread widely among Asian and European countries and caused an economic loss tens of billions of dollars [8]. The various subtypes of avian influenza viruses directly led to the deaths of tens of millions of birds. In addition, to control the spreading of the influenza, hundreds of birds had to be slaughtered and disposed of. Poultry contributes to approximately 20% of the protein consumption in developing countries [9]. Such outbreaks greatly impacted on the poultry industry of the affected countries in terms of decrease in export and loss of consumer confidence, as infectious disease is listed as one of the few reasons authorized by World Trade Organization (WTO) for blocking imports of agricultural products.

Infectious diseases are caused by pathogens. The types of pathogens cover a broad spectrum of basic organisms in microbiology, including virus, bacterium, fungus and parasite. These pathogens work as the agents for infectious diseases when they spread from an infected host individual or group to another susceptible host. The transmission of pathogens can occur through many different routes,

including direct or indirect contact, airborne, blood, or other body fluids. In recent years, increasing human activities such as migration and urbanization have created many new pathways for transmission of pathogens, making the transmission even easier than before [10]. Other factors that facilitate the pathogen transmission include climate change, biodiversity change and nutrient pollution [11].

It is worth noting that co-infections by more than one pathogen strain have become commonplace and can carry greater risk than a single infection. Co-infections have been a contributing factor to the mortality of infectious diseases in developing countries as many assays only test for one agent and miss the presence of a co-infection. One typical example is the co-infection between human immunodeficiency virus (HIV) and hepatitis C virus (HCV). An estimated 2.3 million people living with HIV are co-infected with hepatitis C virus (HCV) globally [12]. Viral hepatitis usually progresses faster and causes more liver-related health problems among people with HIV than among those who do not have HIV [13]. Co-infection can also occur when one pathogen has multiple strains or genotypes. Strains are important because they can differ greatly in many traits, including growth rate, virulence, infectivity, antigenicity and drug resistance [14]. The study of multiple-strain infections can improve the understanding of host-pathogen interactions, disease dynamics, and novel control approaches. And the capability of simultaneously detecting multiple pathogen

strains is highly desirable for a variety of medical researches and clinical applications.

To identify the presence or absence of certain pathogens is the key step for the diagnosis of infectious diseases. Conventional diagnostic approaches often rely on the use of microbial culture and microscopic examination to measure the existence of specific micro-organisms [15]. But culture methods often have low yield and microscopy is relatively insensitive. Such detection requires substantial time, equipment and training, and not all pathogens can be cultured and clearly distinguished from others under microscope. Many other diagnostic approaches involve the use of biochemical tests to indirectly identify the pathogens through measuring enzymes or antibodies that are correlated to particular types of micro-organisms [16]. Emerging novel approaches such as nucleic acid testing and next-generation sequencing are also applied for the rapid and accurate diagnostics of infectious diseases [15]. Generally speaking, the diagnostic methods must be accurate, simple and affordable for the population for which they are intended. Furthermore, considering the communicable nature of the infectious disease and the potential risks brought by the delay of effective treatment, they must provide results in time to allow for the establishment of the following control measures and treatment [17]. For some disease outbreaks, early diagnosis can play a critical role in interrupting the transmission of the pathogens. The ability of rapid detection and timely reporting can greatly improve the current way that the infectious diseases are managed.

1.2 Nucleic acid test

In recent years, the development of molecular diagnostic techniques has brought significant improvements in the diagnosis and monitoring of infectious diseases [18]. The nucleic acid test (NAT), also referred to as nucleic acid amplification test (NAAT), is a molecular technique that has been widely used for the detection of various infectious agents [19]. The NAT diagnosis is able to identify the pathogens through the detecting and amplification of their genomic sequences, known as the target DNA or RNA sequence. The amplification process of the target sequence can generate thousands to millions of copies of the target genomic fragment, making a large amount of nucleic acids. The detection results can be indicated by measuring the fluorescent labels that are designed to bind to the nucleic acids. Compared to traditional diagnostic methods, the NAT technologies offer several advantages. Firstly, NAT is a highly sensitive method since it can detect low levels of DNA or viral RNA. Secondly, the detection is specific since only the target sequences can be amplified. Thirdly, the diagnosis process can be rapid, making it possible to have early treatment of the diseases. Lastly, the NAT diagnostic has the potential of multiplexing detection, the ability to detect multiple pathogens in a single clinical specimen. Currently, there are two major types of NAT approaches: one involves a periodic thermal cycling process and the other involves an isothermal process.

Polymerase chain reaction (PCR) is an *in vitro* enzymatic reaction that can provide large quantities of a specific DNA fragment with the help of repeated thermal cycles under the deriving of DNA polymerase [20]. This easy-to-carry out technique has become a very popular and often indispensable tool in medical and biological laboratories for numerous types of applications, including DNA cloning, DNA sequencing, gene function analysis and the diagnosis of infectious disease. The thermal cycles, comprised of alternating heating and cooling of the reaction, can help the separation and enzymatic replication of the target DNA. During the thermal cycles, the primers, which are short DNA fragments containing the complementary genomic sequence of the target DNA, work with DNA polymerase to generate replicas of the target, in the format of a chain reaction. The process of a classical PCR is illustrated in Figure 1.1. For each PCR cycle, a double stranded DNA (dsDNA) is firstly denatured at a high temperature (~ 95°C) , which can break all the hydrogen bonds between the two strands of the DNA, and create two complementary single strand DNNAs (ssDNA). Secondly, the ssDNAs are annealing at low temperature (~ 55°C) to allow for the binding of the specifically designed primers at the ends of the ssDNA sequence of interest. Finally, the DNA polymerase binds to the primer sites and catalytically elongates the primer to synthesize a new DNA strand complementary to the DNA template at ~ 72°C. Ideally, the number of target DNA copies doubles after each cycle, and the newly synthesized DNAs become the sequence template for the next cycle. Through this kind of chain reaction, the number of target DNA copies can be

exponentially amplified. PCR is traditionally performed in a small reaction tube in a thermal cycler, and the amplified DNAs can be visualized through gel electrophoresis or fluorescent labels [21].

Loop mediated isothermal amplification (LAMP) is a nucleic acid amplification technique that was first reported in 2000 [22]. Compared to PCR, the major feature of LAMP is that it does not need the series of temperature changes, and it can be carried out at a constant temperature. At the LAMP reaction temperature (~60-65°C), the double-stranded DNA is in a "dynamic equilibrium," and the polymerase is prone to both strand displacement activity and replication activity. The detail of the LAMP process is illustrated in Figure 1.2 [23]. Typically, 4 different primers are used in LAMP, which increases the specificity of the LAMP detection, as shown in Figure 1.2a. With the help of the polymerase, the primers anneal to 6 different regions on the target DNA and make the initial elongations (Figure 1.2b). The output of the first stage annealing, elongation and displacement is a dumbbell-like structure with stem-loops at both ends, which also serves as the template for the following cycling amplification steps (Figure 1.2c). In each cycle, one strand is displaced during the elongation with the addition of new loops. The released single strand can form a new stem-loop structure that is complementary to the initial template, and then it uses itself as the template to start the new synthesis. The reaction will stop when the concentrations of the reagents and enzymes become low or the buffer capacity is reached.

Both PCR and LAMP can be used for the detection of RNA targets through the reverse transcription (RT) process, which can create complementary DNA from an RNA template [24].

1.3 Microfluidic devices

The microfluidic technologies have been under rapid development in recent years, and they have become powerful tools in a wide range of biomedical research and applications [25]. Many of the complex laboratory assays performed with expensive and bulky instruments can be miniaturized and performed on an integrated microfluidic system, which is also often called a lab-on-chip (LOC) [26]. Such LOC systems typically consume only small volumes of analytes, provide high sensitivity detection, and can be fabricated from low-cost materials, making it possible to achieve point-of-care (POC) diagnostics, which is defined as analytical testing performed outside the central laboratory using devices that can be easily transported to the vicinity of the patient [27]. The POC feature provided by microfluidic devices is of great importance in resource-limited settings such as developing countries. The miniaturization of laboratory instruments and the simplification of the sample preparation process can allow the development of high-throughput, easy-to-operate, portable and affordable assays that can be accessible to a large group of people, and that are critical to global health applications.

There are currently two major types of microfluidic devices: one type is continuous-flow microfluidics and the other type is droplet-based microfluidics [28]. Continuous-flow is the mainstream operation approach for microfluidic devices because of the easy implementation and the good control of the fluids. The continuous liquid streams in the microfluidic channels are usually driven by external pressure, mechanical pumps, capillary force or electrokinetic mechanism. The droplet-based microfluidics, on the other hand, involve the generation and manipulation of discrete volumes of fluids inside the microfluidic channels. Compared to the continuous-flow microfluidic devices, the droplet-based microfluidic devices are able to manipulate the motion of single dispersed droplets, so as to achieve better control of the fluid volume and perform high throughput analyses. The droplets can be generated by several different methods, for example by utilizing the geometry of microfluidic channels and the electrical properties of the fluids [29].

Microfluidic systems are usually fabricated from silicon, glass, quartz, and various polymeric materials [30]. The fabrication approaches for the microfluidic devices have been extensively studied with the help of the well-established semiconductor fabrication technologies, especially the micro-electro-mechanical-systems (MEMS) technologies [31, 32]. The selection of materials is usually dependent on the specific application of the microfluidic device. Many microfluidic devices are made of polymers such as PDMS (Polydimethylsiloxane) and PMMA (polymethyl methacrylate) because of their good biocompatibility,

low cost and simple fabrication process. PDMS is an optically transparent, soft elastomer that can be easily engineered into various shapes using thermal curing process. But the use of polymer materials is problematic for some fluorescence-based detection due to the strong auto-fluorescence [33]. Glass is another commonly used transparent material but with low auto-fluorescence. Silicon is an opaque material, and has the unique advantage of high thermal conductivity. Glass- and silicon-based microfluidic devices are usually fabricated through photolithography, dry/wet etching and physical/chemical deposition process. Other material properties that are critical to successful application of microfluidic devices include analyte adsorption, permeability, chemical resistance, electrical insulation, and hydrodynamic resistance [34].

1.4 Mobile health

The widespread use of mobile devices has offered a novel approach to address many health-related challenges. The emerging mobile health (mHealth) technologies rely on mobile communication devices such as cell phones and tablets to realize remote medical diagnosis and monitoring [35]. In many regions of the world, medical equipment is either unavailable or insufficiently portable for wide and fast deployment. Meanwhile, the mobile devices and mobile networks can be present in these regions. According to the data released by International Telecommunication Union (ITU), in 2015 96.8% of the people worldwide are mobile-cellular telephone subscribers, and 47.2% of them are active mobile-

broadband users [36]. The penetration of mobile devices in many low- and middle-income countries has surpassed many other infrastructures such as paved roads, electricity, and advanced healthcare resources. Such increasing accessibility of mobile devices can provide opportunities to transform the way health services and information are delivered, collected and managed.

Smartphones have been increasingly adapted in various health care applications in recent years. According to the applications, the use of smartphone-based healthcare practice can be divided into two categories: out-of-clinic use and in-clinic use [37]. Out-of-clinic smartphone use covers most of the software applications (apps) and the corresponding devices for the daily monitoring of the health and wellness. Smartphones can also be used to promote a healthy life style and help people get access to useful medical information when they need it. Built-in sensors inside the mobile devices or external wearable sensors measure people's health-related activities such as heartbeat and breathing during walking, running, or sleeping [38]. Unlike older generations of at-home monitoring equipment that require manual record keeping, these applications usually have a high-level of automation in terms of the recording and processing of the measured data, and usually the information is stored in a personalized profile that can be securely transmitted to a cloud center to perform processional medical analysis. Such applications usually present the data in an appealing graphic fashion to users and provide simple suggestions or conclusions. On the other hand, the in-clinic applications of smartphones involve the diagnostics of specific types of diseases

and are supposed to help make clinical decisions. Many of the tests that are usually exclusively performed in centralized laboratories with high-end instrumentation and skilled personnel can be simplified and realized with the smartphones. For example, a single-channel electrocardiograph (ECG) can be integrated at the back case of an iPhone [39]. A lead I ECG can be generated when patients rest the fingers of both hands on the electrodes on the rear of the cell phone. Although the one-lead ECG is not as comprehensive as the standard twelve-lead ECG for the assessment of heart function, it can perform basic heart monitoring in a quick and easy way. Likewise, plug-and-play blood pressure monitor can wirelessly connect to a smartphone [40]. Instead of simultaneously operating both a stethoscope and sphygmomanometer while diagnosing the patient, the clinician can directly obtain the data collected by smartphone and focus on engaging the patient talking about his or her health status. There are also smartphone-based instruments for microscopy, spectroscopy and solid/liquid phase bio-assays [41]. By utilizing the mobile devices that patients have already purchased for non-medical purposes, whose operation is already familiar for people with non-technical backgrounds, the barrier of accessing millions of medical instruments for the large population of people in resource-limited settings can be eliminated.

Challenges for the current mobile health technologies include the expansion of detection capacity to complex diseases, privacy and security concerns, and the difficulties of regulatory approval [42].

1.5 Figures

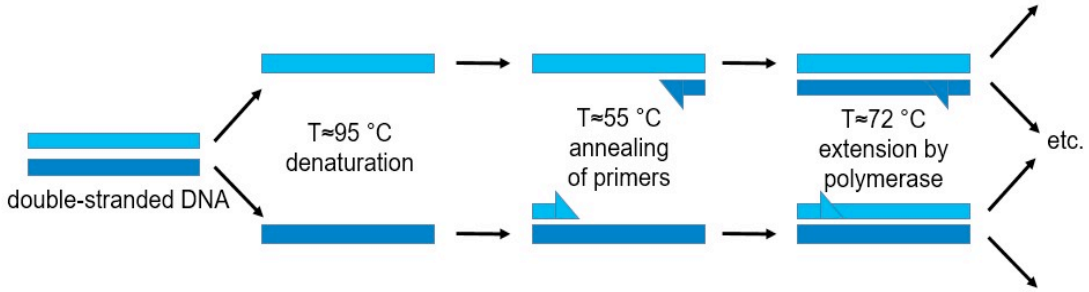

Figure 1.1: Schematic diagram of the classical PCR process.

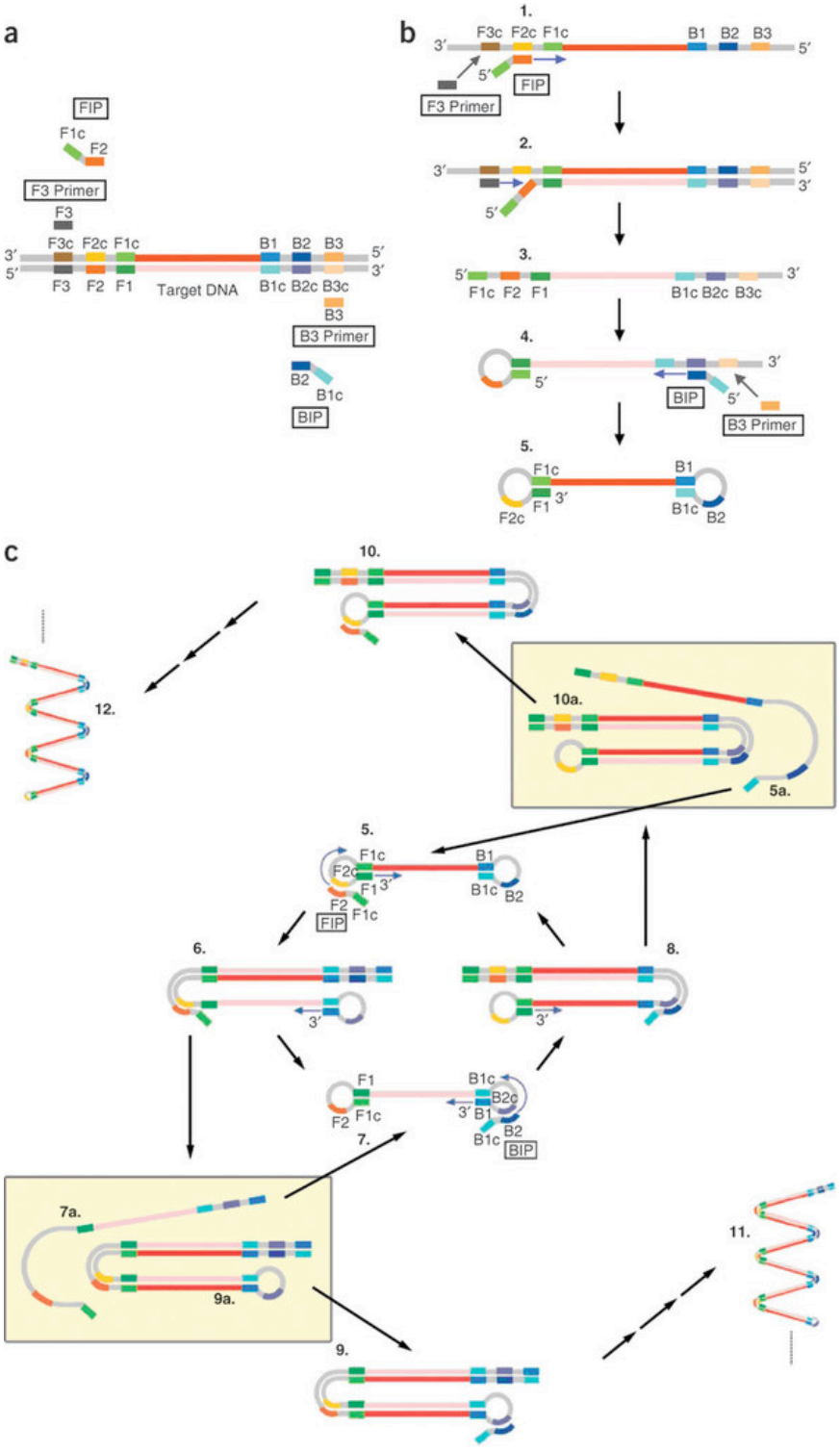

Figure 1.2: Schematic diagram of the LAMP process [24].

CHAPTER 2

SMARTPHONE-BASED SYSTEM FOR HIV DETECTION

2.1 LAMP assay for HIV detection

Human immunodeficiency virus (HIV) affects about 35 million people worldwide [43]. During the course of nearly four decades since the emergence of HIV on a pandemic scale, advances in antiretroviral therapy have transformed HIV infection from a death sentence into a chronic illness which can have little impact on life expectancy for those in whom the infection is properly managed [44]. At the population level, rates of new infections, mother-to-child transmission, and deaths from HIV-related causes are declining. However, the availability of the appropriate diagnostic technologies essential to informing treatment in routine HIV care is still among the chief barriers preventing access to the standard of care for millions of HIV-positive individuals worldwide, particularly in resource-limited settings.

CD4+ T lymphocyte counts and blood plasma viral load are the two core diagnostic measurements broadly considered essential to HIV care, as they both guide the initiation of therapy and indicate the efficacy of each individual's treatment regimen [45]. CD4 counts, traditionally performed by flow cytometry, are increasingly available in remote settings due to the introduction of new portable platforms [46, 47]. Viral load platforms, on the other hand, trail CD4 technologies in penetrating the developing world. Viral load instruments are

traditionally reverse-transcription polymerase chain reaction (RT-PCR), nucleic acid sequence-based amplification (NASBA), or branched DNA (bDNA) assays which require a laboratory setting, extensive sample handling, and sophisticated processing [48].

One promising solution that can help address this issue is loop-mediated isothermal amplification (LAMP) [49]. LAMP emerged in the early 2000s as an alternative to PCR for nucleic acid detection [22]. LAMP is attractive for point-of-care applications because it does not require temperature cycling like PCR (isothermal at 60–65 °C), and because it is typically less sensitive than PCR to amplification inhibitors. Reverse transcription loop-mediated isothermal amplification (RT-LAMP) assays for HIV were first described quickly after the introduction of the initial concept [50, 51], and there have been several reports since then for variations of the assay, including efforts toward point-of-care applications [52, 53]. To date, however, an approach capable of performing a quantitative RT-LAMP assay from a drop of whole blood on a platform compatible with a fully automated, portable device has not been presented.

Traditionally, it is believed that nucleic acid amplification requires complete purification of the RNA or DNA target to be compatible with the amplification reaction. The robustness of LAMP, however, has disrupted this thinking and whole blood treated only with cell lysis buffer has been employed by Curtis et al. for HIV LAMP in a qualitative measurement in an electricity-free heating device [52]. We present here RT-LAMP with minimally processed lysed

whole blood for a quantitative measurement of HIV viral load capable of detecting as few as 3 virus particles per ~60 nL reaction droplet. Our approach to RT-LAMP HIV viral load measurements begins with a drop of whole blood. The data presented here demonstrates the potential of the approach to be developed into a fully automated mobile device that does not require manual processing. We implement a simple microfluidic mixing module to show the whole blood lysis step can be performed on a chip without loss of analyte or interference with the detection assay. We then move to a microchip platform and characterize the RT-LAMP reaction with purified RNA and lysed whole blood spiked with viral RNA, imaging with both a standard fluorescence microscope and a consumer smartphone without hardware modifications. We then integrate the microfluidic lysis, microchip reaction platform, and smartphone imaging to demonstrate the capability of our platform to quantitatively determine HIV viral load from a drop of blood.

2.2 Smartphone-based instrumentation

A Samsung Galaxy Note 4 smartphone was purchased for imaging of the RT-LAMP reaction on the microchip substrate. The smartphone hardware was not modified from its factory conditions. A high-pass colored glass filter with cut-off at 530 nm was placed between the camera and the chip to isolate the fluorophore emission wavelengths. A 3D-printed cradle (Figure 2.1) was designed to position the smartphone horizontally with the camera directly above the microchip. A

mounting cylinder was also 3-D printed to hold a BLUE LED which fit within the cradle and illuminated the microchip from an angle. A mounting cylinder was also 3-D printed to hold a high-output blue light-emitting diode (LED) and a shortpass filter with a 500 nm cut-off wavelength, which fit within the cradle and illuminated the microchip from an angle. The LED was powered with 3 V from an Agilent E364xA DC power supply with automated on/off function controlled with a MATLAB script. It was also determined that the Blue LED could be adequately powered by a standard 3 V lithium coin battery, but the DC power supply was used for the purpose of PC control.

Due to biosafety considerations, the entire smartphone imaging apparatus was placed inside a biosafety cabinet for performing integrated measurements. For this reason, remote control of the imaging function was desired. The Android application IP Webcam23 was downloaded from the Google Play store and installed on the smartphone. This application transmits a live image over the network which can be viewed in real-time in a web browser. The browser interface allowed for control of the smartphone camera's focus, exposure, and gain. Imaging of the RT-LAMP reaction was performed with the following parameters set in the IP Webcam web browser interface: 8X zoom, 99% stream quality, exposure compensation of 4, and "Night vision" function with a gain of 10.00 X and exposure 10. A MATLAB script was written to automate the image capture process. The script was initialized simultaneously with the activation of the heating stage. The MATLAB script imaged the reaction in the following

manner: blue LED was switched on, delay 3 s, capture image from IP Webcam web browser interface, delay 2 s, and finally switch off blue LED. This process was repeated every 30 s while each reaction was imaged.

A silicon microchip was used for RT-LAMP experiments. Briefly, a silicon wafer was thermally oxidized to create a silicon oxide layer of ~150 nm. The oxide is then patterned with photolithography and hydrofluoric acid etch step, exposing the silicon where the wells will be etched. The wafer was then immersed in a heated Tetramethylammonium hydroxide (TMAH) bath for 18 hours to anisotropically etch the silicon, creating inverted square pyramids for later use as reaction wells. Chips for all on-chip RT-LAMP experiments were prepared in the following manner: First, the microchip was cleaned in a piranha solution containing 1:3 30% hydrogen peroxide and sulphuric acid for 10 min and then rinsed in deionized water. Each chip was then degreased with acetone, methanol, and isopropanol and dried by blowing with nitrogen gas. To produce a hydrophobic surface to promote stability of droplets, the chip was rinsed with Sigmacote® from Sigma-Aldrich by pipetting the solution repeatedly over the surface of the chip. The chip was then rinsed briefly with isopropanol, dried by blowing with nitrogen, and placed in a copper bowl.

A Narishige IM-300 Microinjector with Eppendorf VacuTip microinjection holding capillary (15 μm inner diameter, 100 μm outer diameter) was used both to spot primers and place reaction droplets. A 20 ms injection pulse was used resulting in a droplet of approximately 60 nL. The microinjection

procedure was performed after chip cleaning and preparation as follows: LAMP DNA primers in TE buffer were diluted in water to the final reaction concentration. Droplets were placed in all 36 wells of the microchip array using the microinjection system and a 3D micromanipulator (MCL-D331) from World Precision Systems. The process was visualized with a Leica MZFLIII microscope. Droplets containing primers were allowed to dry completely, leaving dehydrated DNA LAMP primers in the reaction wells. Following visual confirmation that all droplets had dehydrated, the chip was submerged in heavy mineral oil (Fisher) and placed in a desiccator to remove air bubbles. The primary function of the mineral oil is to protect the reaction droplets from evaporation during heating at 65 ºC.

During degassing, the primer-less RT-LAMP reaction was prepared and transferred to the microinjection capillary. Reaction droplets were then placed in each well by lightly contacting the bottom of each reaction well, injecting a droplet of approximately 60 nL, and lifting the capillary out of the oil. The chip containing all 36 droplets submerged in oil in the copper bowl was then transferred to the heating stage and imaging apparatus (fluorescence microscope or smartphone apparatus).

2.3 Experiment results

The samples used in this experiment were whole venous blood samples that were drawn from HIV-negative donors with a syringe and HIV-1 IIIB virus

propagated in the H9 human T lymphocyte cell line. HIV-1 RNA was purified from HIV-1 IIIB whole particles using the PureLink® Viral RNA/DNA Mini Kit from Life Technologies. The master mix of RT-LAMP contains reaction buffers, enzymes, and primers. Viruses were spiked into lysed blood following the mixing to keep the virus concentration identical between samples.

The RT-LAMP was demonstrated on a microchip in a microfabricated silicon micro-well array. All on-chip RT-LAMP measurements were prepared with DNA LAMP primers pre-spotted and dehydrated on the chip prior to oil immersion, degassing, and reaction droplet placement. Initially, purified RNA in water was characterized on the chip. Figure 2.2a displays fluorescence curves measured with a fluorescence microscope, while Figure 2.2b shows the threshold time analysis. Threshold time for each individual reaction was approximated from baseline-subtracted fluorescence curves by determining the measurement time at which the signal exceeded 20% of the maximum fluorescence value it achieved during the course of the entire measurement. In this measurement, data from 6 droplets total were removed due to outlying behavior believed to be due to contamination, experimenter error, or because no reaction was observed. The analysis includes one of six reactions in each of the 10^2-10^3 (yellow) and 10^1-10^2 (green) vp/RXN samples, and four of six reactions in the 10^0-10^1 (blue) vp/RXN sample. In Figure 2.2c-f, lysed whole blood spiked with viral RNA was imaged with the smartphone apparatus as described in the experimental section. Whole viruses were not used in this measurement as the apparatus had not yet been

converted to be contained within a biosafety cabinet. Figure 2.2c shows fluorescence curves gleaned from the smartphone images, Figure 2.2d shows the threshold time analysis, and Figure 2.2e shows examples of the smartphone fluorescence images every minute for minutes 7-11. Four of the six reactions for the sample at approximately 10^1 vp/RXN (green) were omitted because they did not react before 30 min. Figure 2.2f shows an endpoint measurement obtained following termination of the real-time monitoring at 30 min. Four additional droplets in the array had reacted before the image in Figure 2.2f-i was captured with the fluorescence microscope. Figure 2.2f-ii is an additional smartphone image captured shortly after the microscopy image was obtained. Figure 2.2f-iii is identical to Figure 2.2f-ii with an additional overlay color-coded consistent with the color-concentration convention used throughout this work, from left to right: red for concentrations of 10^4-10^5 vp/RXN, orange for 10^3-10^4, yellow for 10^2-10^3, green for 10^1-10^2, and blue for 10^0-10^1 vp/RXN. The sixth column on the far right is a negative control containing blood sample and reaction mix without viral RNA. Finally, Figure 2.2f-iv is a colormap rendering of Figure 2.2f-ii produced in MATLAB as an example of the image analysis process.

Integrated experiments were designed to demonstrate the full capacity of this approach for a sample-to-answer solution to point-of-care HIV viral load quantification. The complete flow of the experiment is depicted in Figure 2.3a. These experiments differed from other measurements presented in this work in that whole blood samples were spiked with “live” HIV-1 IIIB virus particles (not

viral RNA) at a range of concentrations and each individual sample was analyzed on a separate chip. Of the 36 wells on the micro-chip array, 6 were used for negative controls and up to 30 were used to test the sample.

Five samples were tested (named A-E), containing approximately 32,000, 3,200, 320, 32, and 3.2 virus particles per reaction, respectively. Since each reaction droplet contains approximately 4.8 nl of whole blood, this corresponds to viremias in the range of $6.7 \times 10^5 – 6.7 \times 10^9$ viruses per mL of blood, or $1.3 \times 10^6 – 1.3 \times 10^{10}$ RNA copies per mL of blood plasma (assuming 45% haematocrit).

Due to biosafety considerations, the entire process was adapted as described in the experimental section to be contained within a biosafety cabinet. This introduced challenges to droplet placement, which was performed with a motorized micromanipulator controlled with a joystick and guided by a video feed from a small table-top microscope. Decreased control over droplet placement led to a decreased success rate in droplet placement. As a result, not all of the thirty wells designated for a virus-positive reaction droplet were used in every measurement. The number of successfully placed droplets for samples A through E was as follows: 29, 28, 30, 22, and 22.

Figure 2.3b shows the fluorescence curves, measured with the smartphone system, for all droplets which amplified within 30 min. Figure 2.3c shows the threshold time vs. virus number. The slope of the fit to threshold time vs. virus number is -1.9993, which differs in magnitude by 98.0% compared to on-chip

RNA in lysed whole blood, 13.9% compared to on-chip RNA in water, 18.5% compared to virus particles in whole blood in the thermocycler, and 25.9% compared to purified RNA in water (method 2) analysed in the thermocycler. In Figure 2.3d, we consider a new metric, which is amplification efficiency, and observe a trend between virus number and the fraction of droplets which amplified. A framework for understanding this phenomenon in the context of digital LAMP measurements is described in the next section.

The replacement of laboratory hardware (e.g. thermocycler fluorescence detection or fluorescence microscope) with a common smartphone is a core aspect of the novelty of this research. First, it demonstrates that the lysed blood RT-LAMP measurement can be performed with existing mobile technology that is at least as affordable as a high-end smartphone. Furthermore, trends suggest that mobile communications technologies will continue to improve in capabilities and decrease in cost, an exciting outlook for fluorescence and other optics-based point-of-care diagnostics. Second, our platform, consisting of a 3-D printed platform, LED light source, emission filter, and small form-factor heating stage suggests that, if adequately robust, an add-on component may be developed as an attachment to existing smartphones, shifting the computation and imaging burden from components integrated with the diagnostic platform to a consumer item that is becoming ubiquitous, even in resource-limited settings [54]. This could significantly reduce the production and deployment costs of such a technology.

2.4 Figures

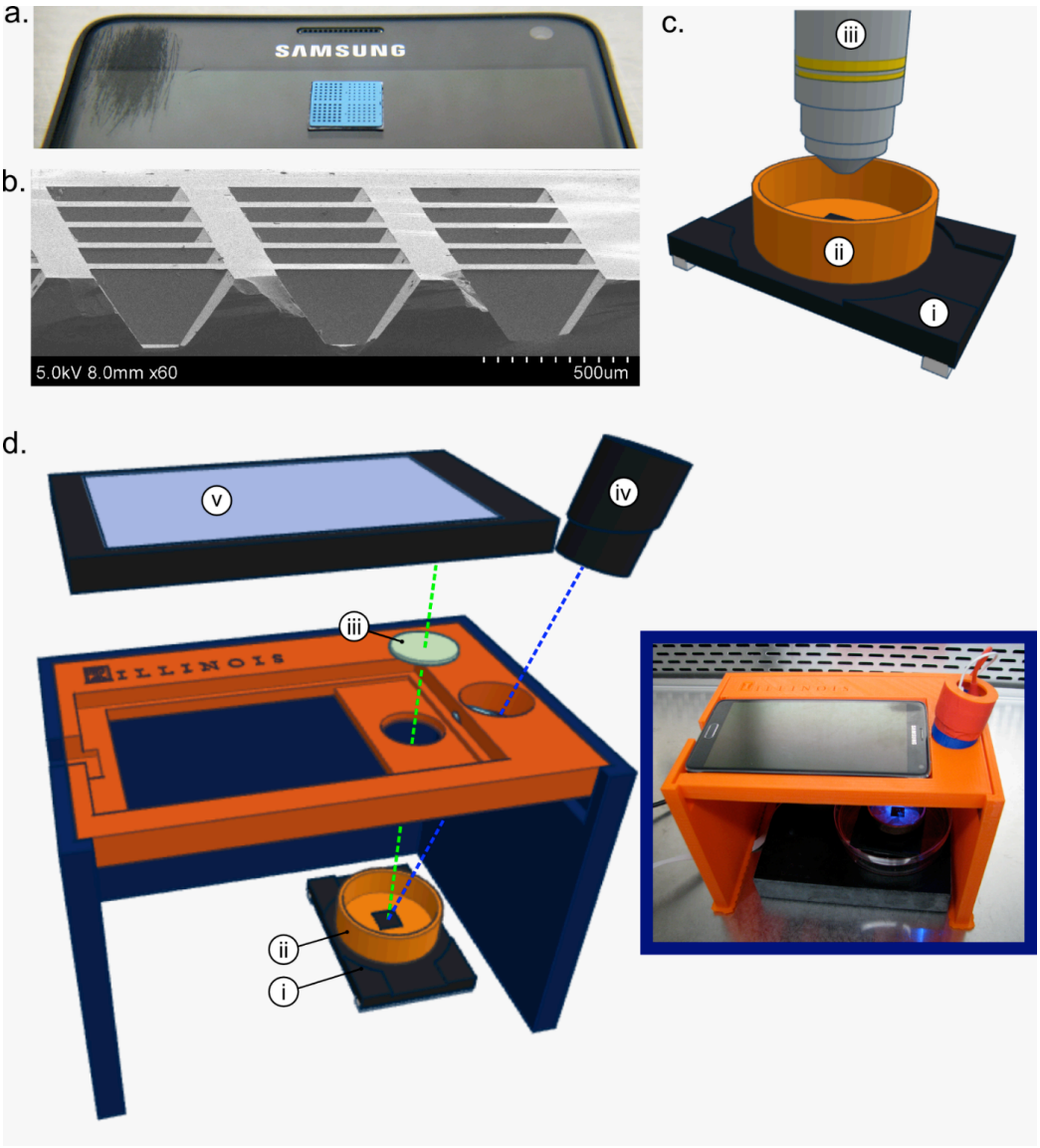

Figure 2.1: The instruments for smartphone-based HIV detection.

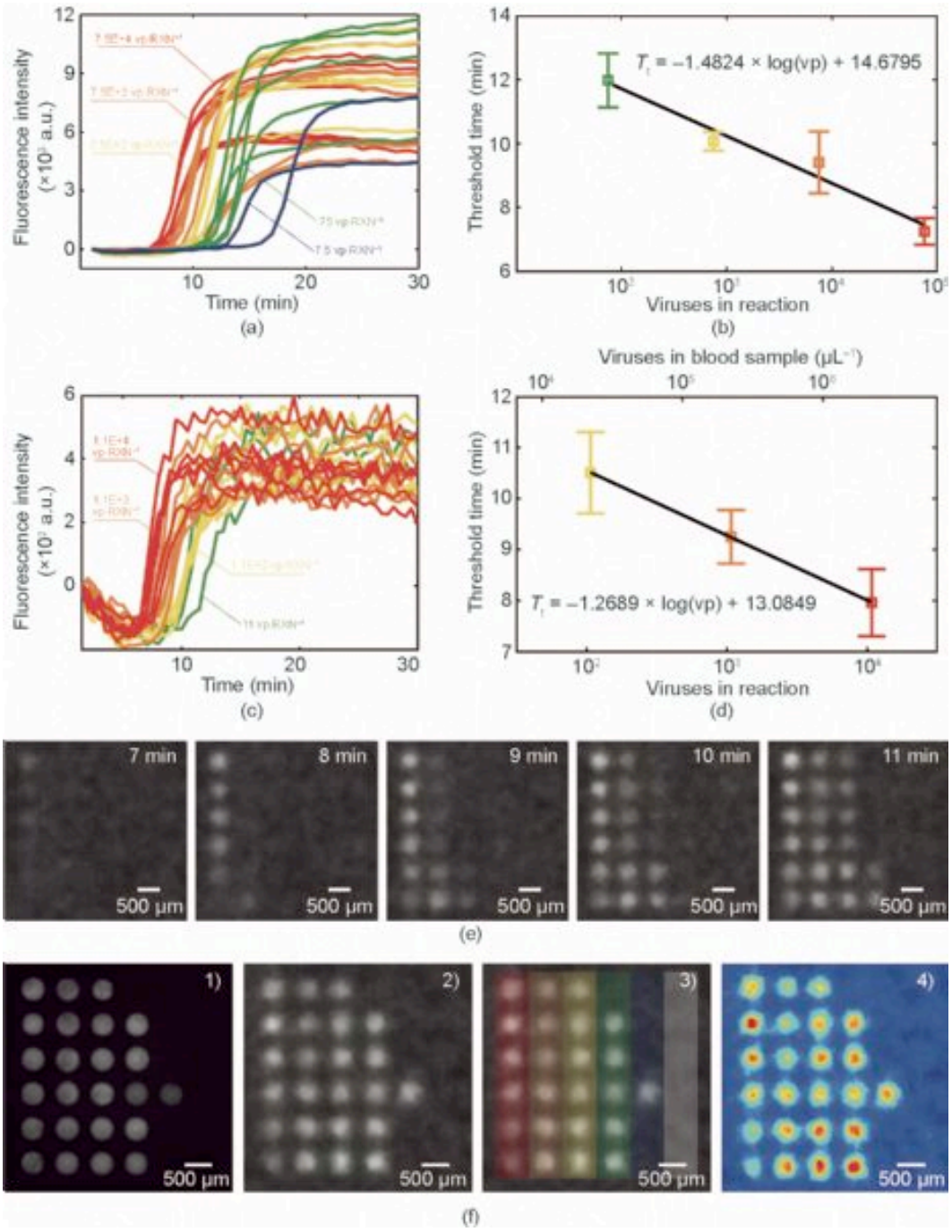

Figure 2.2: On-chip RT-LAMP for HIV-1 detection using smartphone.

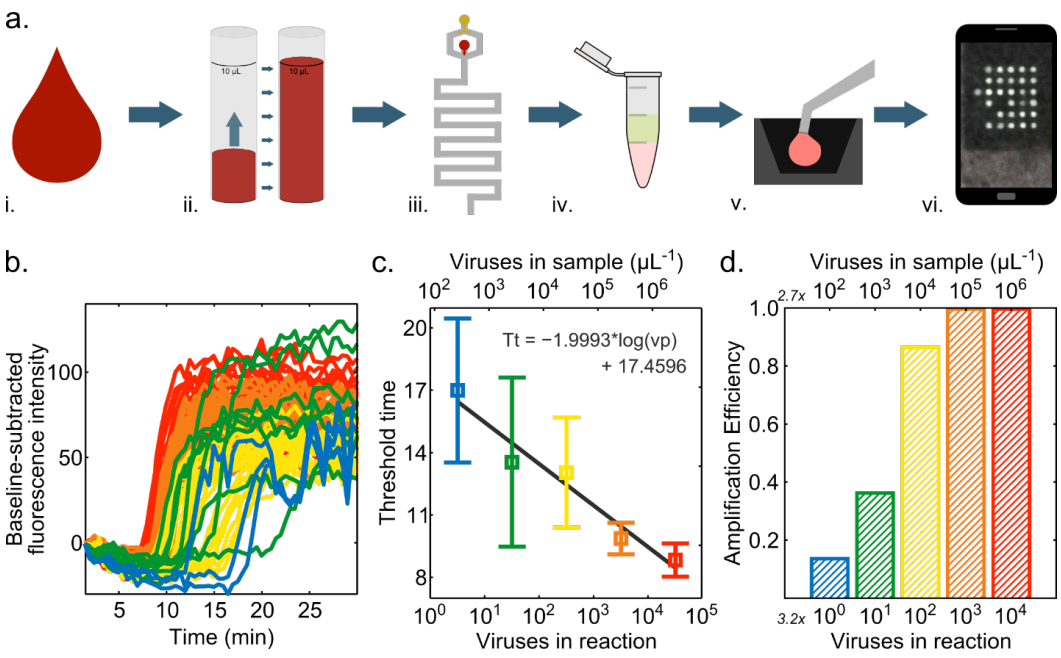

Figure 2.3: Integrated RT-LAMP detection of HIV-1 in lysed whole blood.

CHAPTER 3

SMARTPHONE-BASED SYSTEM FOR MULTIPLEXED DISEASE-SPECIFIC NUCLEIC ACID SEQUENCES DETECTION

3.1 Introduction

Infectious diseases, such as HIV/AIDS, tuberculosis, and malaria, while accounting for less than 10% of deaths in the developed world, are responsible for more than half of all deaths in developing countries [2]. A contributing factor to the mortality of infectious diseases in developing countries is that co-infection by more than one pathogen carries greater risk than a single infection, while many assays that only test for one agent could miss the presence of a co-infection. Despite recent progress in the development of new drugs for treatment of viral, bacterial, and fungal infections [55], the worldwide death toll continues to rise with critical needs for increased understanding of fundamental disease mechanisms, and enhanced point-of-care diagnostics. Importantly, there is a need for improved surveillance tools that can detect the emergence of drug-resistant strains, alert clinicians to the initiation of a potential outbreak, monitor the effectiveness of quarantines, and facilitate cross-communication between clinicians that are geographically distributed. For human infectious diseases in the US, approximately 55 are designated as “reportable” by the Centers for Disease Control, which requires a positive laboratory test to be communicated to central authorities, enabling the information to be reported to clinicians by the National

Notifiable Diseases Surveillance System (NNDSS), which is most heavily utilized only for the most deadly disease outbreaks [56]. Most forms of influenza have no reporting requirement, and thus no information is currently gathered or communicated for human respiratory infectious diseases that are responsible for 2-3 million cases and 250,000 – 500,000 deaths worldwide each year [57]. Reporting requirements are even more rudimentary in the developing world, leaving clinicians largely unaware of the global view of incidence, spread, and control of infectious disease that affects their community.

The societal and economic toll of infectious disease is not limited to human populations. Animals raised for human consumption live in facilities in which large herds share ventilation, feed, and waste handling within confined spaces in which respiratory infectious disease can spread rapidly. Similar concerns exist for companion animals and racing animals, particularly for those with high economic value. In veterinary medicine in the US, only a handful of infectious diseases are categorized as "reportable" by the USDA, requirements vary from state to state, and no cross-communication infrastructure exists that enables veterinarians to easily share results with each other.

A key characteristic for a successful system for detection and reporting of infectious disease is speed. For example, modeling studies on various intervention strategies for pandemic influenza response have shown that the highest impact on attack rate is obtained by identification and initiation of treatment one day earlier [58]. Particularly for point-of-care scenarios, where the

clinician is testing a patient at a remote clinic, a farm, or a racetrack, the need to send samples to a central laboratory, to wait for the test to be performed, and to wait for the results to be reported, results in an enormous waste of opportunity to determine if aggressive treatment or quarantine is needed before the disease spreads further. The ability to rapidly share the results of positive and negative tests can revolutionize the manner in which infectious diseases are managed. Therefore, it is of paramount importance for the test to be performed at the same location as the patient, so action can be taken within the same day as the sample is gathered.

Taking advantage of the fact that bacteria and viruses have distinct genetic components that are represented by unique nucleic acid sequences, the most commonly used laboratory analysis technique used for diagnosis of infectious disease is the Polymerase Chain Reaction (PCR) [59-61]. PCR enables sequence-specific concentration amplification of infectious disease DNA through a series of thermally cycled chemical reactions between a set of enzymes, a prepared test sample (of DNA extracted from a pathogen-containing bodily fluid), and disease-specific "primer" molecules. PCR primers for detection of every common human and animal infectious disease have been identified, and may be inexpensively synthesized through readily available commercial sources. Conventional PCR amplification requires expensive laboratory-based instruments that are operated by technicians and housed in central facilities, although there have been strong efforts aimed at miniaturization of PCR for translation closer to the point of care

through the engineering of systems integrated into a small chip or cartridge [59, 61-89]. Many of these efforts have aimed at accelerating the thermal cycling process through reduction in the liquid volume [70, 74, 79, 80, 83, 85, 88, 90-93], while others have explored various modalities for sensing the presence of the amplified product using biosensors [94-98]. Due to the cost and complexity of implementing thermal cycling (generally between 95 °C (denaturation), 72 °C (extension), and 68 °C (annealing) with ~30-40 cycles), various isothermal nucleic acid amplification methods have been proposed and demonstrated with comparable sensitivity to PCR [99-101], but with a requirement to more fully customize and validate the primer sequences. Of these, loop-mediated isothermal amplification (LAMP) has emerged as a compelling approach for portable applications [102-104]. Details of the LAMP process, primer design, and example applications are thoroughly explained in [105].

An important prerequisite for the widespread adoption of point-of-care (POC) tests is the availability of detection instruments that are inexpensive, portable, and able to share data wirelessly over the internet [106-110]. Due to the rapid development of computational, communication, and sensing capabilities of smartphones since the introduction of the iPhone in 2007, these devices have become similar to personal computers with integrated cameras, geolocation capabilities, and access to cloud services. Since 2011, over 478 million smartphones are sold annually, with that number expected to double in the next 4 years [111], making them a nearly

ubiquitous tool that can be adapted to performing POC tests. Recent examples include attachments that enable smartphones to serve as stethoscopes [112], ultrasound probes [113], microscopes [114], fluorescent microscopes [115, 116], label-free biosensor detection instruments [117, 118], fluorimeters [119], and colorimetric assay readers [120]. Portable detection systems for infectious disease are already recognized as a likely extension of mobile technology [102, 121-126], and a PCR or LAMP mobile sensing platform that is integrated with a smartphone and a smart service system for reporting and sharing results with a network of users is highly desirable.

In this work, we have developed a smartphone-based portable detection instrument to perform isothermal LAMP-based analysis for the diagnosis of equine respiratory infectious diseases. While our ultimate goal is the diagnosis and mobile reporting of human infectious diseases, we initially focus specifically upon equine respiratory infections due to their economic importance to the horse racing industry, similarity to the tests that would have an impact upon the food animal industry, and the strong need for a service system that can inform networks of field veterinarians. Our work involves the development of a microfluidic approach for identifying the presence of specific nucleic acid sequences from the pathogens of equine respiratory infections using a portable detection system integrated as a disposable cartridge that can be read by a conventional smartphone in conjunction with a custom-designed cradle. Capable

of simultaneously performing 10 parallel isothermal amplifications (with two utilized for experimental controls and eight for pathogen-specific DNA detection assays), the system can detect target DNA sequences from more than one pathogen with a single test protocol, and interface with a smartphone app that communicates with a cloud-based service for the immediate reporting of the location, time, identity, and results (positive and negative) of the detection. In this paper, four LAMP-based assays have been developed for the detection of four important equine respiratory infectious pathogens: streptococcus equi (S. Equi), strangles (streptococcus zooepidemicus, abbreviated as S. Zoo), equine herpesvirus type 1 and type 4 (EHV-1 and EHV-4). The smartphone-based detection demonstrates the same detection limits and sensitivity as LAMP reactions performed on commercially available laboratory-based systems, and is capable of identifying the specific nucleic acid sequences of pathogens for both single-infection and co-infection scenarios. To our knowledge, a smartphone-based nucleic acid testing approach for the diagnosis of veterinary infectious diseases has not been reported in previous literature.

Our approach utilizes a silicon microfluidic chip with LAMP primers applied to individual assay lanes, which is embedded within a credit card format plastic holder to facilitate handling and to carry assay-specific information. The chip accepts a single droplet (~15 μL) test sample that is distributed between 10 separate regions. After a ~30 min LAMP reaction (conducted on a hotplate, separate from the phone), the plastic card is inserted into a slot in the body of a

cradle (in the same manner as chip readers used for modern credit cards) that places the chip in contact with a heater from below, while illuminating with LEDs from above. The cradle accepts an unmodified smartphone, placing the chip in front of its rear-facing camera, which gathers a fluorescent image of the assay lanes through a macro lens (to increase field of view) and an optical emission filter. Image processing software operating on the smartphone automatically recognizes the regions of interest within the fluorescence image that correspond to the relevant assay lanes, and determines a fluorescent intensity value for the positive control, negative control, and each assay. The system reports normalized fluorescent endpoint intensity values of each lane and generates a positive/negative determination for each assay in ~5 s. The software application operating on the smartphone gathers information about the tests conducted on the microfluidic card, patient-specific information, and results from the assays that are communicated to a cloud storage database. Although not the focus of the results presented here, the database anticipates queries from a network of geographically distributed users who seek updates when positive tests are recorded within user-defined constraints (such as geographic area, disease, animal category, or date) and the ability to graphically represent trends such as temporal sequences of positive tests overlaid with location, and trends over time. We anticipate that a smart service system for clinicians would also facilitate messaging between users to easily share information such as specific circumstances of tests and the outcomes of treatment. Integration of a

smartphone-based testing capability and smartphone-based epidemiology capability represents a future goal of the sensing capability reported here.

3.2 Experimental

3.2.1 Chip substrate fabrication

To perform multiplexed LAMP detection of pathogen-specific nucleic acids, a silicon-based microfluidic chip with 10 parallel flow channels and a shared sample inlet was designed and fabricated. The chip is the size (25 mm × 15mm) of a standard SIM (subscriber identity module) card. Flow channel dimensions are 10 mm in length, 500 μm in width and 200 μm in depth, representing a volume of 1 μL each. The inlet of the chip is a 4 mm entrance chamber that feeds its contents to 10 parallel assay channels. Two square markers at the opposite end of the chip are used for position alignment during fabrication and for automated image recognition during the assay measurement. The fabrication process for the microfluidic chip is illustrated in Figure 3.1a. A 4-inch <100> silicon wafer (University Wafer, South Boston, MA) with one side polished is thoroughly cleaned and used as the substrate in the photolithography process. Positive photoresist SPR 220 (MicroChem, Newton, MA) is spin-coated on the polished side of the wafer to form a 4.5 μm covering layer, followed by a soft-bake at 60 °C for 2 min and 110 °C for 1 min. The photoresist is then exposed with an i-line (365 nm) mask aligner (EVG 620) with an expose dose of 180 J/cm^2. The

exposed regions of the photoresist with the outline of the microfluidic pattern are subsequently removed by immersing the wafer in AZ developer diluted 1:4 with deionized (DI) water for ~4 min. The photoresist in the unexposed regions is solidified though a hard-bake at 110 °C for 1 min. For the anisotropic etching of the silicon substrate, a Bosch process with alternating steps of SF_6/O_2 etching and C_4F_8 passivation is used to create 200 μm deep trenches in an inductively coupled plasma reactive ion etcher (ICP-RIE). After the Bosch process, the remaining photoresist was stripped with acetone and O_2 plasma cleaning, leaving the bare silicon exposed. Because bare silicon has been reported to have inhibitory effects on nucleic acid amplification due to absorption of polymerase [61], the wafer was thermally oxidized in a furnace (1150 °C) for 2 hours to grow a 200 nm film of SiO_2. The final step of the chip fabrication is to dice the wafer into individual chips (Figure 3.1b). The scanning electron micrograph (SEM) in Figure 3.1c shows the vertical sidewalls of the etched channels.

3.2.2 Chip preparation and sealing

Before preparing them for assays, microfluidic chips are stored under vacuum in a desiccator after being thoroughly cleaned with piranha solution, a mixture of 98% sulfuric acid (H_2SO_4) and 30% hydrogen peroxide (H_2O_2) at the ratio of 3:1, rinsed with distilled water (DI) and then dried with nitrogen gas. For the on-chip experiments, an adhesive membrane and a glass coverslip are used to prevent evaporation of the reaction solution in the flow channels during heating at 65 °C.

The chip is covered with a transparent double-sided adhesive (DSA) (ARseal™ 90880, Adhesives Research) with laser-machined holes after the deposition of primers into the channels. The holes are cut to match the position of inlets and ends of the channels at the substrate, to allow for displaced air venting during injection of the test sample. The holes are also used to inject LAMP primers individually into each lane, as discussed in section 3.2.3. Figure 3.1d shows the deposition process for the four types of primers and two experiment controls. The DSA forms a barrier to evaporation or cross-contamination, and it is compatible with the reagents used in the amplification reaction. After the reaction solution is injected into the channels, the chip is sealed with a glass coverslip (GOLD SEAL® 63760-01, Electron Microscopy Sciences) by peeling off the top covering layer of DSA and binding it with the coverslip. The binding is robust enough to effectively prevent the entrance of air into the flow channels from the surrounding environment.

The chip is housed within a plastic laminated holder that is in the shape of a credit card (85.6 mm × 54.0 mm × 0.8 mm). The holder is designed to handle the small microfluidic chip during the measurement on the smartphone-based instrument preventing the user from touching the chip, and to provide a surface upon which barcoded information about the included assays can be printed. Polyoxymethylene (POM) is selected as the card material because of the low auto-fluorescence, low cost, and excellent dimensional stability. After the on-chip amplification reactions start and reach the plateau stage, the chip is placed inside

the card and loaded into the cradle for the scanning of the quick response (QR) code and for the multiplexed reading of 10 assay lanes. Information about the on-chip detection including the serial number of the chip, primer deposition date and assays in each channel can be provided by the holder card.

3.2.3 Primer deposition

The primers are uniformly deposited onto the surfaces of the flow channels before sample loading through the pipette injection at the endpoint of each channel. Channel 1 serves as the positive control by depositing a mixture of the primer set and template DNAs for S. Zoo, while channel 2 serves as the negative control because no primers are deposited within it. The remaining eight channels are divided into four groups to allow for the deposition of four types of primer sets used in this work, with channels 3 and 4 prepared with primers for the S. Equi assay, channels 5 and 6 deposited with primers for the S. Zoo assay, channels 7 and 8 deposited with primers for the EHV-1 assay, and channels 9 and 10 deposited with primers for the EHV-4 assay. The primer solution injected into the eight channels is prepared with a direct 20-fold dilution of the corresponding primer solution (originally at 55μM) in nuclease-free water, giving a final primer concentration of 2.75 μM. For the solution injected in the positive control channel, 1 μL of the S. Zoo DNA sample solution at a concentration of 5×10^6 copies/mL is mixed with 1 μL of 20 times diluted 55μM S. Zoo primer solution to make a 2 μL final solution. After the solutions are prepared, a volume of 1 μL of

each solution is taken by a pipette and injected into the corresponding flow channels from the end of each channel. The injected liquids flow along the etched trench reaching the opposite end of the flow channel without entering the common inlet hole. Due to the small volumes, all the primers completely dry on the channel surface at room temperature within a few minutes. The primer deposition process enables batches of chips to be prepared in advance and stored for later use.

3.2.4 LAMP assay development

We have developed four specific LAMP assays to demonstrate the functionality of the smartphone-integrated instrument for the multiplexed detection of pathogen-specific nucleic acid sequences. Streptococcus Equi (ATCC® 9528™), Streptococcus Zooepidemicus (ATCC® 39920™), Equine Herpesvirus-1 (USDA 040-EDV), and Equine Herpesvirus-4 (USDA 044-EDV) were chosen as the pathogens of interest due to their widespread virulence among horse populations. The S. Equi and S. Zoo bacteria are received in lyophilized form and are propagated in bovine-brain heart infusion medium (Sigma Aldrich) for a period of 16 hours to obtain a carrying concentration of 1×10^{8} colony forming units (CFU)/mL. Glycerol stocks are prepared from this concentration and are stored at -80 °C until needed for experiments. The Equine Herpesvirus-1 and Equine Herpesvirus-4 stocks are aliquoted into smaller volumes and also stored at -80 °C until needed. DNA from all the pathogens are extracted via a standard heat-lysing

protocol as described earlier [127]. The extracted DNA is quantified using PCR standard curves that were established using synthetic targets.

A 25 µL LAMP reaction mix contains the following: 3.5 µL of 10mM dNTPs (New England Biolabs), 2.5 µL of 10X Isothermal Amplification Buffer (New England Biolabs), 2 µL of 5M Betaine (Sigma Aldrich), 1.5 µL of 100 mM Magnesium Sulfate Solution (New England Biolabs), 2 µL of primer mix, 2 µL of 8000units/mL Bst 2.0 Warmstart DNA Polymerase (New England Biolabs), 1.25 µL of 20X Evagreen Dye (Biotium), 2.25 µL of DEPC-treated water (Invitrogen), and 8 µL of the template DNA. The LAMP reactions are validated on a benchtop thermocycler (Eppendorf Realplex Thermocycler) at 65 °C for 40 min and terminated by heating at 85 °C for 5 min. The 25 µL reaction mix is divided into three equal parts (8 µL) for triplicate repetition. Ten-fold serial dilutions of the extracted DNA are carried out in DEPC-treated water to determine the working range of our LAMP assays.

Novel LAMP primers were designed for S. Equi and S. Zoo, targeting the *seM* and *sorD* genes respectively. The target sequence for S. Equi was obtained from the NCBI database using GenBank AJ249868.1 and U73162.1. The target sequences for S. Zoo were also obtained from the NCBI database using GenBank CP002904.1, NC_011134.1, and FM204884.1. LAMP primers were designed using Primerexplorerv4 (https://primerexplorer.jp/e/). LAMP primers for EHV-1 and EHV-4 were utilized from the sequences reported by Nemoto et al [128]. All LAMP primers were synthesized by Integrated DNA Technologies (IDT DNA)

and are listed in Table 3.1. Briefly, each primer mix consists of 0.2 μM of F3 and B3, 1.6 μM of FIP and BIP, and 0.8 μM of Loop F and Loop B primers.

3.2.5 Smartphone-based instrument

The smartphone-based instrument to measure the fluorescent emission from the on-chip LAMP reactions is shown in Figure 3.2. The system consists of a smartphone phone (Nexus 6; Motorola, IL, USA) and a 3D-printed plastic cradle body that contains the optical and electrical components to excite and collect fluorescence signals at a constant, controlled temperature. The top part of the cradle interfaces with the rear-facing camera of a Motorola Nexus6 smartphone (13 megapixels, pixel size of 1.4 μm). The cradle aligns the smartphone camera with the internal optomechanical components, and also serves as a dark chamber for fluorescence detection by excluding external light. A schematic of the fluorescence imaging system is depicted in Figure 3.2a. When the mobile phone is slid into the slot at the top of the cradle, the rear-facing camera is aligned over a window (30 mm) that is formed by a long pass filter (525 nm, Edmund Optics, #84-744) and a macro lens (12.5X, TECHO, #TECHO-LENS-01) in series. The long pass filter is selected according to the emission wavelength of the fluorescent dye used in the LAMP assay. The macro lens placed in front of the camera facilitates close-up photography of the chip, allowing the reduction of the distance between the camera and the chip to 50 mm while keeping the field of view as large as 24 × 24 mm with negligible barrel distortion. A light source module

composed of eight blue light-emitting diodes (LEDs; λ_{peak} = 485 nm, view angle: 135°, luminous flux: 45 lm/W, Cree Inc., #XPEBBL) and four short pass filters (490 nm, Asashi Spectra, #ZVS0510) that cover each pair of LEDs is installed at the upper corners of the cradle to provide the excitation illumination that does not spectrally overlap with the dominant fluorescence emission wavelengths. The LEDs are mounted on a custom-built printed circuit board (PCB) and arranged with square symmetry to support uniform illumination over the whole chip area. The light source module is powered by two AAA batteries and operated using an on/off control switch. A positive temperature coefficient (PTC) heater (12V-80 ˚C; Uxcell, Hong Kong, China) is placed beneath the chip, maintaining the chip 65 ˚C without an additional temperature controller. The PTC heater is made from specific ceramic materials that have a highly nonlinear thermal response and a positive thermal coefficient of resistance. When the temperature of the heater exceeds a composition-dependent threshold, the electrical resistance increases resulting in decreased heat output to set the temperature at a predefined limit. The installed PTC heater is powered by a standard 9 V battery to set the temperature of the microfluidic chip around 64~ 66 ˚C during the measurements and operated using an on/off control switch. The overall dimensions of the cradle are ~ 90 × 70 × 95 mm^3. The purpose of the PTC heater is not to provide thermal energy for the LAMP reaction, but to maintain the chip at an elevated temperature during fluorescence imaging, in which fluorescent background intensity is reduced compared to room temperature, which increases signal-to-background

measurement of the LAMP assays. Thus, extended heating and precise temperature control are not required. The cost of the components used to construct the instrument is approximately $550, and the system weight is approximately 15 ounces, not including the phone.

3.2.6 Fluorescence microscopy

To verify correct performance of the LAMP assay by an independent instrument, fluorescence microscopy was used to capture the real-time images of the on-chip LAMP reactions under a Nikon Eclipse FN1 fluorescence microscope with a 2× objective and a Nikon 96311 B-2E/C FITC fluorescence filter. While the smartphone assay reader is intended only to measure assay endpoints, the fluorescence microscope enables real-time visualization of the LAMP reaction. For fluorescence microscopy analysis of the chip, the sealed chip is placed on an INSTECT mK1000 heating stage located under the microscope objective. The field-of-view of the objective is large enough to measure the fluorescence output from only six channels of the microfluidic chip at the same time. NIS Elements software provided by Nikon is programmed to capture fluorescence images at 1 min intervals with 9.6× gain and 1 s exposure time.

3.2.7 Image analysis and app development

The fluorescence images of the chip are captured by the smartphone in JPEG format, for analysis by an Android app developed to support this project. The

image is comprised of a 3120 × 4160 × 3 matrix. The first two dimensions represent the size of the image, and the last dimension provides a 24-bit RGB (red, green, blue) color space. The RGB intensity components for each pixel are stored as an 8-bit unsigned integer ranging from 0 to 255. Since the fluorescence emission from the microfluidic chip is green, centered at λ=530 nm, only the G channel intensity is used in the following image processing. The region of interest for each of the 10 lanes can be derived through a boundary detection method (Figure 3.3) [129-137]. Within each lane's region of interest, covering a span of 40×700 pixels, the average and standard deviation of all the pixel intensities are calculated. The average intensity obtained from the negative control (lane 2) indicates the background intensity. Due to a combination of factors that include the weak fluorescence of unbound dye and the unfiltered reflected light, the intensity measured in the negative control lane is used as a baseline that is subtracted from the measured output intensity of all the other lanes. The image processing performed by the app reduces each lane to a single intensity value, representing the average fluorescent intensity within the region of interest, minus the average fluorescent intensity of the negative control lane.

The series of images measured by the fluorescent microscope were saved as grayscale TIFF files. These images were imported into Matlab as a 1024×1280 matrix of 16-bit unsigned integers (range 0-65535). Limited by the field-of-view of the objective, only six of the ten lanes can be monitored at once as shown by Figure 3.4. The average pixel intensities in the regions of each lane are calculated

and recorded. Since the image frames are taken at 1 min intervals, the variation of the average intensities of the six lanes can be plotted as a function of time to generate the fluorescence amplification curves.

3.3 Results

3.3.1 Off-chip characterization of the LAMP assay

In order to determine the limit-of-detection for the four developed LAMP assays and to validate the specificity of the primers to the target DNA sequences, the LAMP reactions were characterized in a standard benchtop thermocycler apparatus (Eppendorf MasterCycler RealPlex4). The thermocycler carries a fast 96-well heating block and utilizes fixed 96 LEDs to generate light for fluorescence excitation. Figure 3.5 (a-d) shows the baseline-subtracted amplification curves for the off-chip LAMP assay of S. Equi, S. Zoo, EHV-1, and EHV-4 using purified DNA templates, in which a series of target DNA concentrations spanning 3 to 6 log concentration range were tested one at a time. For the test at each concentration range, the LAMP reaction mixture was allocated into three thermocycler tubes to replicate the detection with a volume of 8 μL in each tube. The lower limits-of-detection are 5×10^4 copies/mL for S. Equi, 5×10^3 copies/mL for S. Zoo and EHV-1, and 1×10^3 copies/mL for EHV-4. Considering the volume of each reaction channel is 1 μL, there are only 1-10 genome copies of the DNA template in the reaction at the limit-of-detection. Target DNA sequence with the concentration below the limit-of-detection cannot be detected through the

amplification reaction. A good linear fit was observed for assays between the log of the target DNA concentration and the threshold time of the amplification, which was recorded as the time taken for an amplification curve to reach 20% of the maximum intensity, indicating good amplification efficiency of the LAMP assays. To demonstrate the specificity of our LAMP assays, which is critical to the multiplexed on-chip detection, each of the four target DNA sequences were tested against non-specific primer sets (Figure 3.6). Specific template-primer amplification is observed for all four assays. The results are summarized in Table 3.2.

3.3.2 On-chip characterization of the LAMP assay

Figure 3.7 (a-e) summarizes results from on-chip characterization of the S. Zoo LAMP assay. The fluorescence microscope was used to monitor the reactions within six channels in real-time for 60 min after introduction of the test sample to the inlet of a primer-prepared chip. We initially performed a negative control test as shown in Figure 3.4a, where deionized (DI) water was used as the test sample, and no S. Zoo DNA were included in the reaction reagents. As shown in Figure 3.4a, no amplification occurs. Similarly, no amplification was observed with a DNA concentration at 5×10^3 copies/mL (Figure 3.4b). When the DNA concentration increases to 5×10^4 copies/mL, all 6 lanes are observed to start amplification reactions within 60 min, and 3 of the 6 lanes reach saturated fluorescent response by 30 min. Therefore, we estimate that the limit of detection

for the on-chip S. Zoo LAMP assay is 5×10^4 copies/mL. As the DNA concentration is further increased to 5×10^5 and 5×10^6 copies/mL, all the lanes provide uniform amplification within 20 min, as shown in Figures 3.4 (d-e). The identical protocol was performed to characterize the on-chip detection limit for the S. Equi, EHV-1 and EHV-4 assays (Figure 3.8, Figure 3.9, and Figure 3.10), for which we obtained detection limits of 5×10^4 copies/mL, 5×10^3 copies/mL and 5×10^3 copies/mL, respectively. This set of experiments shows that the on-chip LAMP assay, measured via the smartphone instrument, provides similar detection limits as the same assay performed in the conventional off-chip format, using a commercially available instrument.

3.3.3 Detection of target DNA sequence in the presence of non-target sequences

The following experiments were designed to demonstrate the ability of this approach to detect viral and bacterial DNA in the presence of interfering non-target DNA. Four types of primers used in the four developed LAMP assays and the positive control mixture were deposited within the microfluidic channels according to the method described in section 3.2.3. Here, we utilized eight assay wells to detect four target DNA sequences, with two replicate lanes for each sequence. When pathogen-specific target DNA sequences are present in the sample injected into the microfluidic chip, the corresponding two channels as well as the positive control channels will generate an amplification reaction with

associated fluorescent emission, while the other lanes remain dark. By measuring the fluorescence output from each channel using the smartphone-based instrument and the software application, detection results can be quickly analyzed and displayed.

Figure 3.11 shows the results for the four experiments performed for the detection of each of the four types of pathogen-specific DNA sequences. For the experiment shown in Figure 3.11a, the sample loaded into the chip contains 5×10^7 copies/mL of S. Equi DNA. As seen in the fluorescence image, lanes 3 and 4, where the S. Equi primers are located, become as bright as the positive control (lane 1). To quantitatively analyze the fluorescence image, the average intensities of the ten lanes, as processed in the method described in section 3.2.7, are calculated. Here, we designate a threshold value, half of the intensity of the positive control, as the value that is used to differentiate a positive test (target DNA present) from a negative test (target DNA not present). As shown in the bar graph in Figure 3.11a, only the intensities of lane 3 and 4 are significantly higher than the threshold, while the intensities of all the other lanes are well below the threshold. The variation in the intensities of the negative lanes for lanes 5 to 10 is due to the difference in the background intensity of LAMP assays and the spatial variation of LED illumination. The error bar in the figure represents the standard deviation of the pixel intensities within each lane. Similar experiments were performed with the target DNA sequences from the other three pathogens. In Figure 3.11b, the concentration of the injected S. Zoo DNAs is 5×10^6 copies/mL.

In accord with the prediction, after the on-chip reactions, lanes 5 and 6 stand out clearly. Figure 3.11c and Figure 3.11d show the detection results for detection of target DNA sequences from viral pathogens EHV-1 and EHV4. Both experiments show clear evidence that the presence of target DNA can be specifically identified without inducing amplification in non-target lanes. The concentrations for the injected EHV-1 and EHV-4 DNAs were 5×10^6 copies/mL and 2×10^6 copies/mL respectively. Application of the thresholding criterion enables the system to differentiate positive from negative results in each lane.

3.3.4 Detection of co-infection with two target DNA sequences present in the same sample

Due to the increased risks brought by co-infections and the fact that the same clinical symptom can be caused by infections from several agents, a POC test which can simultaneously detect multiple pathogen-specific target sequences from a single specimen is highly desirable [27]. To further demonstrate the mobile genetic detection platform, we sought to introduce two target DNA sequences into the same test sample, and to detect positive response from only the corresponding lanes in the microfluidic chip. The sample prepared for this experiment contains 4×10^4 copies/mL EHV-1 DNAs and 3.2×10^5 copies/mL EHV-4 DNAs, while the microfluidic chip is prepared as described previously. Results from this test are shown in Figure 3.12. As shown by the fluorescence image captured by the smartphone, the high-intensity lanes can be clearly identified as lane 1, the

positive control; lanes 7 and 8, which indicate the presence of EHV-1 DNA; as well as lanes 9 and 10, which indicate the existence of EHV-4 DNA. The lanes corresponding to the positive targets are significantly brighter than the negative control and the non-target lanes, and the thresholding method is able to differentiate between positive and negative results.

3.4 Discussion

As described in the Introduction, an important application for the technology platform presented in this work is for mobile diagnostics of pathogen-induced equine disease. Respiratory disease is common in horses and difficult to diagnose using the current methods available to practicing veterinarians. Currently there is little to no monitoring of the health of horses even though they are the most valuable of livestock. Some respiratory conditions such as inflammatory airway disease (IAD) and interstitial lung disease are poorly understood [138] although animals are predisposed to these conditions by viral and bacterial infections [139], which occur worldwide [140]. Miniaturized and portable DNA analyses have emerged as promising tools for veterinary infectious diseases. State-of-the-art miniaturized systems that perform DNA amplification reactions can be classified as: small thermo-cyclers with integrated photodiodes [64, 141], microfluidic systems with customized optics for automated and multiplexed experiments [102, 142, 143], and systems based on electrochemical principles that achieve miniaturization by removing optical elements [144, 145]. Small thermos cyclers

like ‘Palm PCR’ [141] let the user perform the reaction in a pocket-size device, but all the sample preparation is still performed by the user and there are no multiplexing capabilities. The microfluidic ‘FilmArray’ [142] system is highly automated and considerably reduces sample preparation and handling. However, the current technology is expensive, and a large footprint results in a bench-top system unsuitable for portable applications. Electrochemical-based systems like the one demonstrated by DNA Electronics [144] monitor variables like pH change or secondary redox reactions to assess DNA amplification without optical elements. However, these alternatives require the compartmentalization of reactions since the monitoring variables are not specific to the target complicating assay multiplexing.

In general, miniaturized DNA amplification systems seek to minimize footprint, automate processes, and reduce cost without sacrificing sensitivity and specificity of the assay [146]. Additionally, especially for infectious disease detection, it is desirable to have multiplexed assays that enable the screening of multiple agents in a single assay and it is important to create data networks to quickly analyze and share information to contain outbreaks. The devices referenced above fulfill some of these characteristics, but there is no system with all the desired features. The system that we describe in this work is tailored to fulfill the desirable characteristics for portable detection of infectious disease. For example, cost reduction is achieved by performing data acquisition, analysis, and broadcast using a smartphone instead of customized hardware. Also, the use of

preloaded microfluidic cartridges minimizes hands-on labor or required training. The goal of the detection system is also simplified to perform endpoint detection (i.e. not "real-time" PCR), and to provide only positive/negative output for each assay (rather than to estimate DNA copy number). All of the engineering and design parameters in our system can allow for the rapid detection of infectious agents with a mobile instrument that is capable of communicating information with a network of users. Importantly, the technology developed in this project is applicable to detection of any human infectious disease without modification to the sensor chip or the detection instrument through incorporation of human-specific LAMP, and implementation of a sample preparation protocol compatible with blood, urine, stool, or other sample matrices.

The most useful capability for a mobile veterinary laboratory and for human POC diagnosis is to simultaneously test for the presence of more than one pathogen with a single test protocol, which lowers cost, saves time/effort, and allows for a panel of pathogens, which may cause similar symptoms, to be identified. Multiplex LAMP or PCR assays using multiple primer sets in the same reaction can decrease the consumption of sample and reagent but is limited in detection sensitivity caused by uneven amplification efficiencies of the different primer sets [27]. The approach developed in this project splits the initial sample into multiple parallel flow channels for the multiplex LAMP-based detection. It takes less than 30 min to complete the on-chip amplification reactions, and the

existence of specific pathogens can be clearly identified through the brightness of the corresponding lanes on the smartphone-captured fluorescence images.

The incorporation of a smartphone in the detection platform not only reduces the cost of the detection system but also makes it possible to establish a mobile network for the infectious disease epidemiology. The detection results can be collected by the smartphone app and transmitted through the mobile network for the reporting of the pathogens or further analysis at centralized laboratories. Due to the portability of the smartphone-based system, the detection can be quickly deployed and performed in a wide range of regions upon the outbreak of infectious disease, especially in resource-poor environments. On the other hand, the same regions or countries, where the public health system has broken down, often face the highest risk of the emergence of new and once-controlled infectious diseases. A low-cost, portable and smartphone-integrated system provides a promising solution to address the challenges of infectious disease diagnostics in resource-limited settings.

The smartphone-based detection system demonstrated here for identification of specific DNA sequences extracted from the pathogens of equine respiratory infectious diseases represents a significant step towards a practical solution to infectious disease diagnostics in resource-limited settings, and the establishment of a reporting network for infectious diseases. We envision that the detection system can be further optimized for field application and mobile infectious disease detection. Here, we intentionally choose to utilize an

inexpensive and commercially available DNA extraction kit to prepare the sample-to-detect since such kits are already portable and easily available. Because many inhibitors to the amplification-reaction are present in the sample from the respiratory tract, which can cause false-negative results, the extraction kit can help improve the accuracy of the detection [147]. The DNA extraction process is readily translatable to microfluidic formats to generate highly purified DNA for subsequent analysis, and it can be integrated into the same chip along with the DNA amplification and detection [148-150]. As for the further development of this research project, we envision a user in the field starting with unprocessed samples such as nasal swabs or throat swabs that are directly collected from the horses and then injecting the sample into the microfluidic chip for the sample-in and answer-out detection. The detection platform present here is clinically meaningful since the concentrations of the purified DNA detected through the system are all within the clinical range for the four types of pathogens [147, 151]. Importantly, the system is designed to provide a positive/negative determination of the presence of specific pathogens as a promising tool for early-stage disease detection. For the diagnosis of a suspect infection at early-stage, the main interest is to determine the presence or absence of virus or bacteria, while quantification is not strictly necessary. Such determination is valuable to the veterinary practitioners for the early reporting of and precaution against emerging infectious diseases. Based on the positive detection result of the smartphone-based instrument as well as other clinical signs, the detected sample can be sent to a

centralized laboratory or other disease administrator for further detailed diagnostics.

3.5 Conclusion

We demonstrate a smart, mobile, and low-cost service system for the detection of DNA sequences of viral and bacterial pathogens of equine respiratory infectious diseases. The system utilizes a microfluidic approach for performing LAMP-based isothermal amplification of a multiplexed array of 1 to 10 pathogen-specific nucleic acid sequences, and uses a hand-held cradle that interfaces with the rear-facing camera of a conventional smartphone to capture the fluorescence images. The captured images are analyzed by a smartphone app and shared to a cloud-based center for rapid reporting of the detection results. Four LAMP assays have been developed for detection of the specific genes of four major pathogens that cause equine respiratory infectious diseases, including S. Equi, S. Zoo, and equine herpesvirus types 1 and 4. As compared with the assays performed on the bench-top thermocycler apparatus in centralized laboratories, the detection sensitivity is not compromised using the microfluidic approach and the smartphone-based instrument. Importantly, the system is capable of detecting four types of target genomes at the same time to identify the presence or absence of the corresponding pathogens that can cause infection, and also to meet the challenges in diagnosing co-infections of multiple pathogen strains. By generating a positive or negative determination of the existence of specific pathogens, the mobile system can

inform treatment and quarantine responses for the detected infectious diseases that are currently not possible with tests performed at central laboratory facilities. We believe this approach provides a mobile, simple and inexpensive capability for clinicians to perform infectious disease diagnostics, and it represents a significant stride towards a practical solution to infectious disease diagnostics in resource-limited settings.

3.6 Figures and Tables

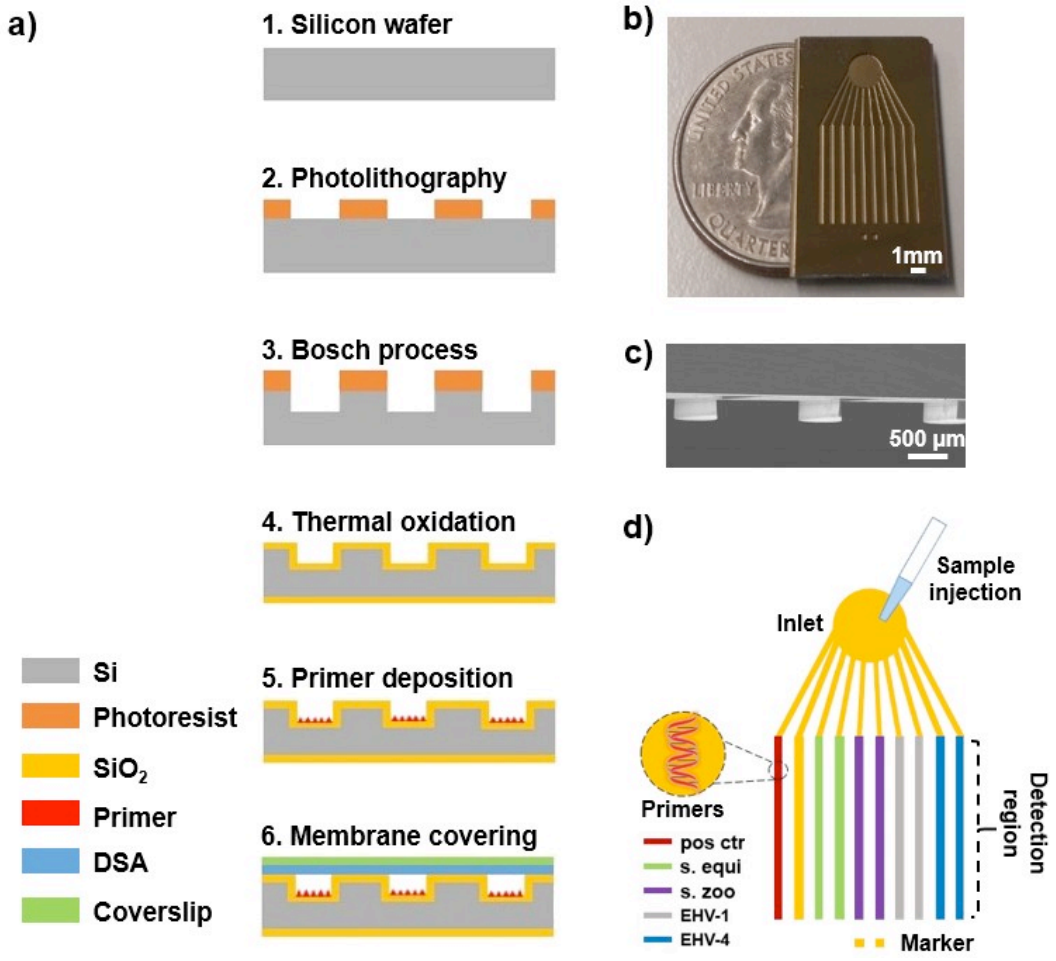

Figure 3.1: Ten-flow channel microfluidic chip for multiplexed LAMP detection. a) Schematic diagram of the fabrication process for the microfluidic chip. b) Photo of a fabricated chip taken with a US quarter. c) Scanning electron microscope (SEM) of the cross-section of the microfluidic channels. d) Primer deposition plan for the on-chip reactions.

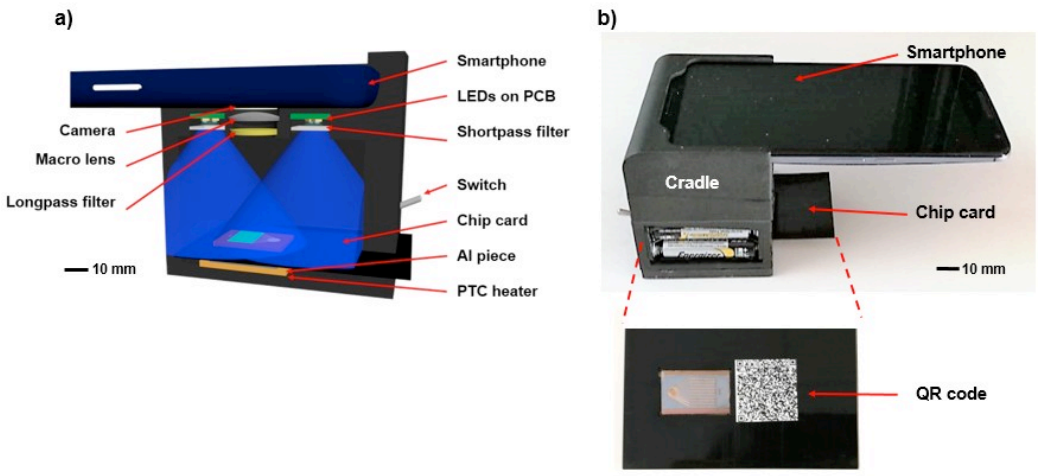

Figure 3. 2: Smartphone-based instrument. a) Schematic diagram to show the internal structure of the cradle that integrates optical and electrical components used for smartphone fluorescence microscopy. The microfluidic chip, integrated in its card, is inserted into the cradle that incorporates a PTC heater to maintain a constant ~ 65 °C temperature. b) Photo of the smartphone-based instrument taken with the smartphone and chip card. A QR code label is printed on the chip card to provide information about the on-chip detection.

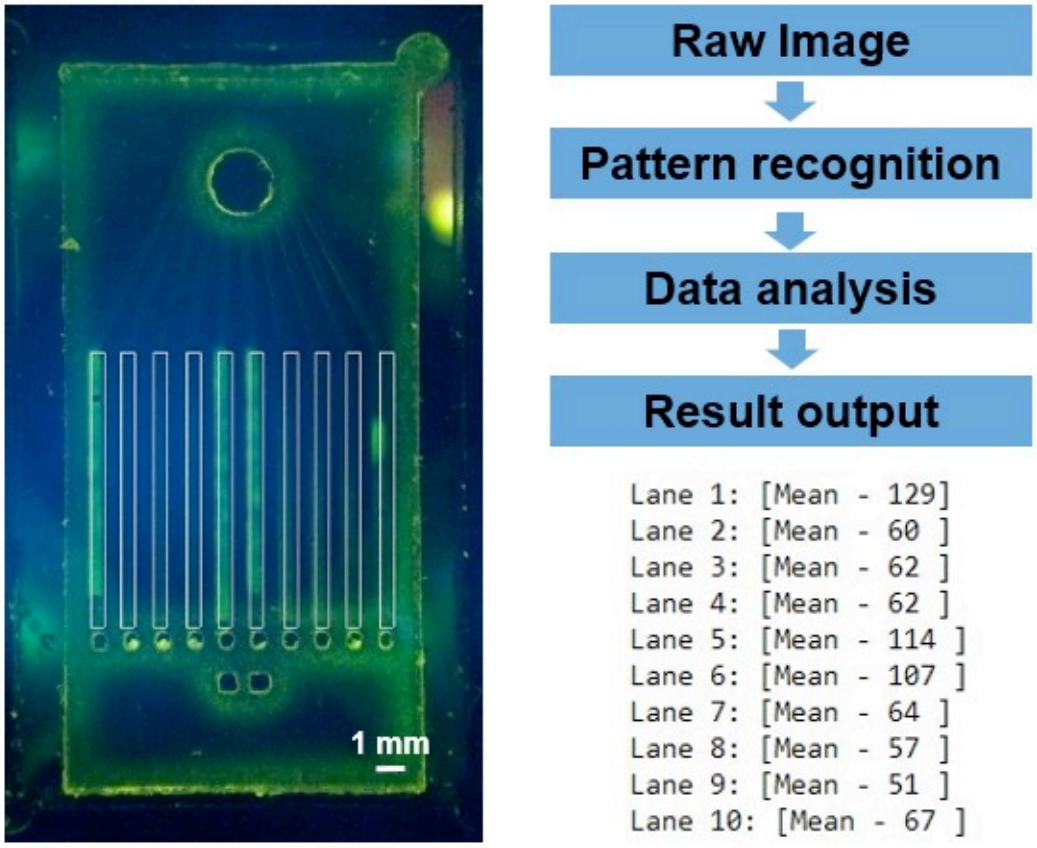

Figure 3.3: The smartphone app developed for the recognition of the microfluidic channel regions of interest and the calculation the of the green pixel intensity of each channel.

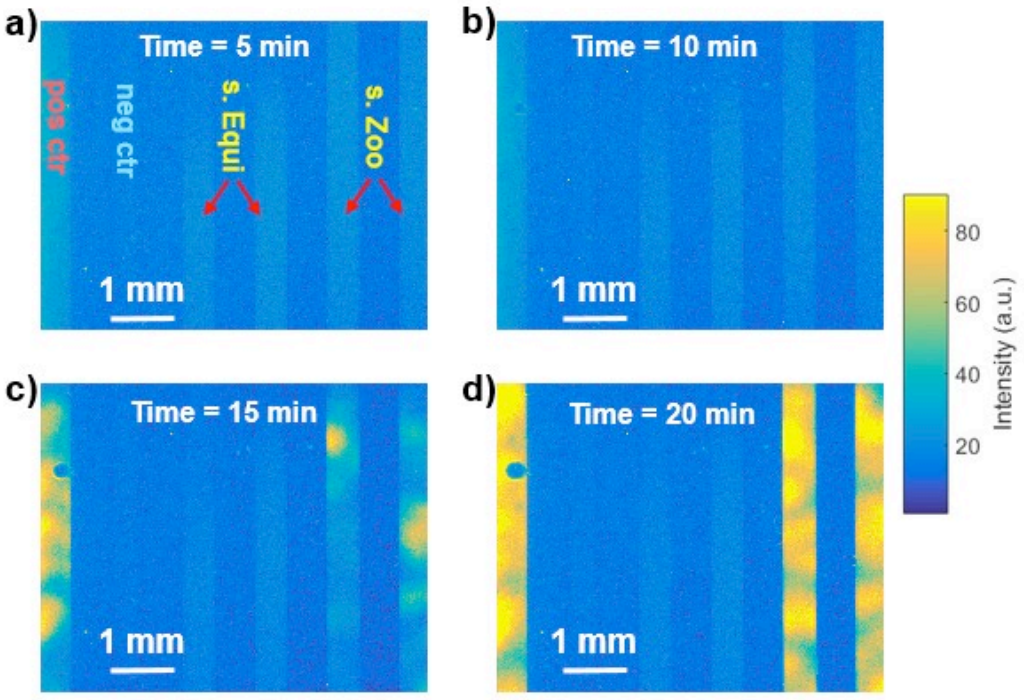

Figure 3.4: Real-time measurement of the on-chip reactions when the sample contains only S. Zoo DNA. The images were captured at 1 min intervals using the fluorescence microscope. The images captured at a) 5 mins, b) 10 mins, c) 15 mins, and d) 20 mins are shown here. Only the positive control and channels deposited with S. Zoo primers become bright.

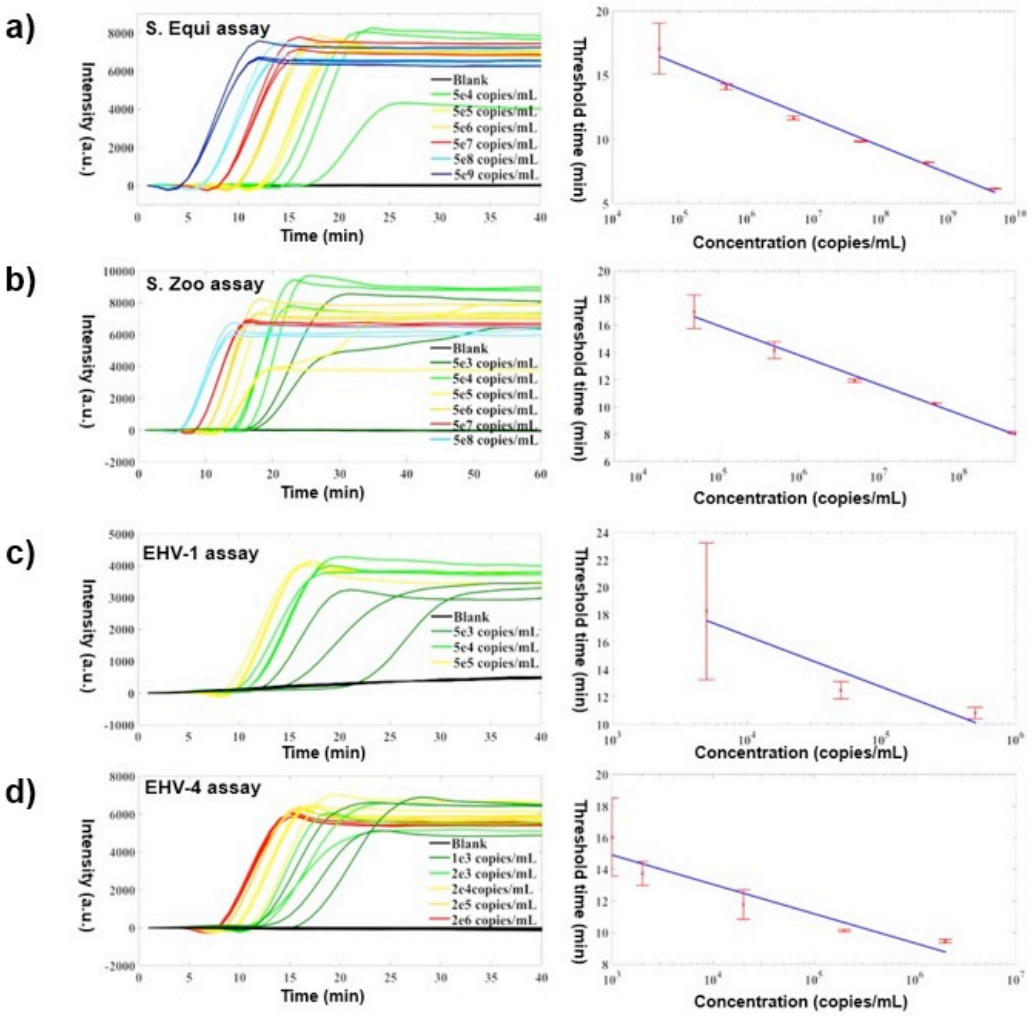

Figure 3.5: Off-chip characterization of the four LAMP assays developed for the detection of equine respiratory infection pathogen DNA. The amplification curves and threshold time versus concentration relationship are plotted for a) S. Equi, b) S. Zoo, c) EHV-1, and d) EHV-4.

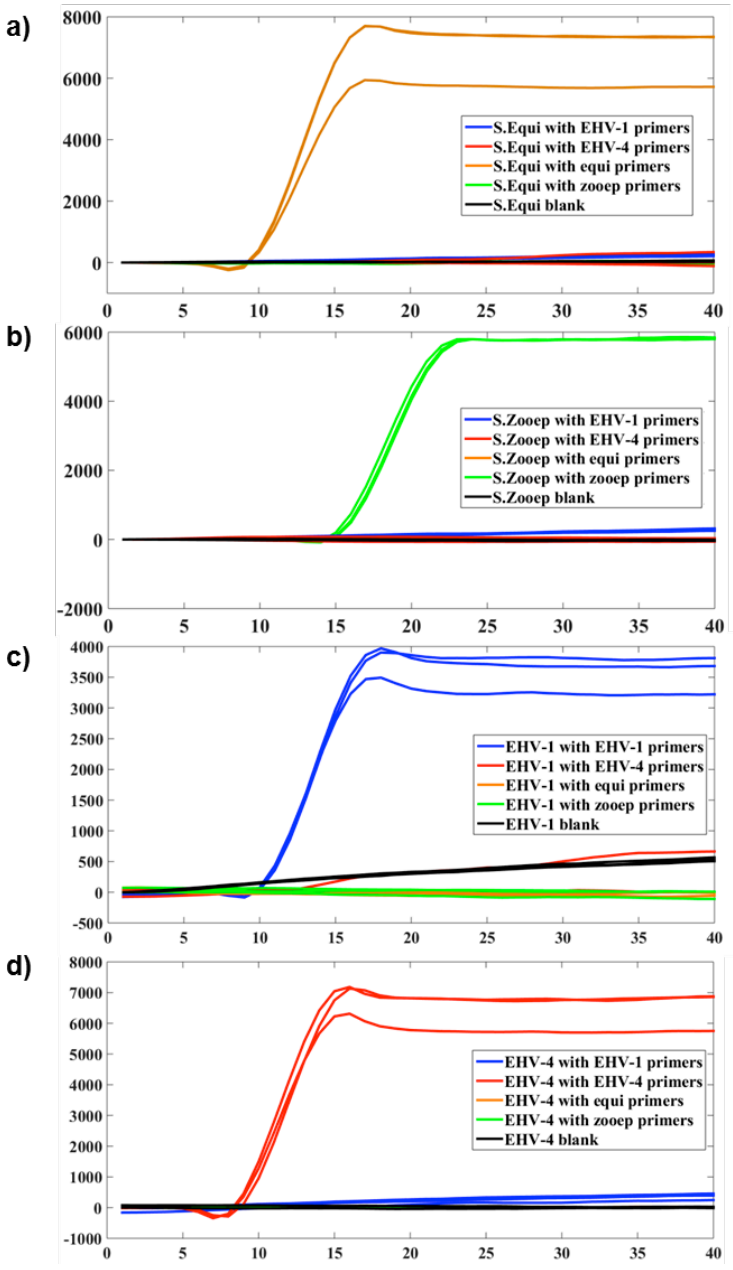

Figure 3.6: Off-chip verification of assay specificity. The real-time reaction curves of a) the S. Equi DNA, b) S. Zoo DNA, c) EHV-1 DNA and d) EHV-4 DNA with all four primers and negative control.

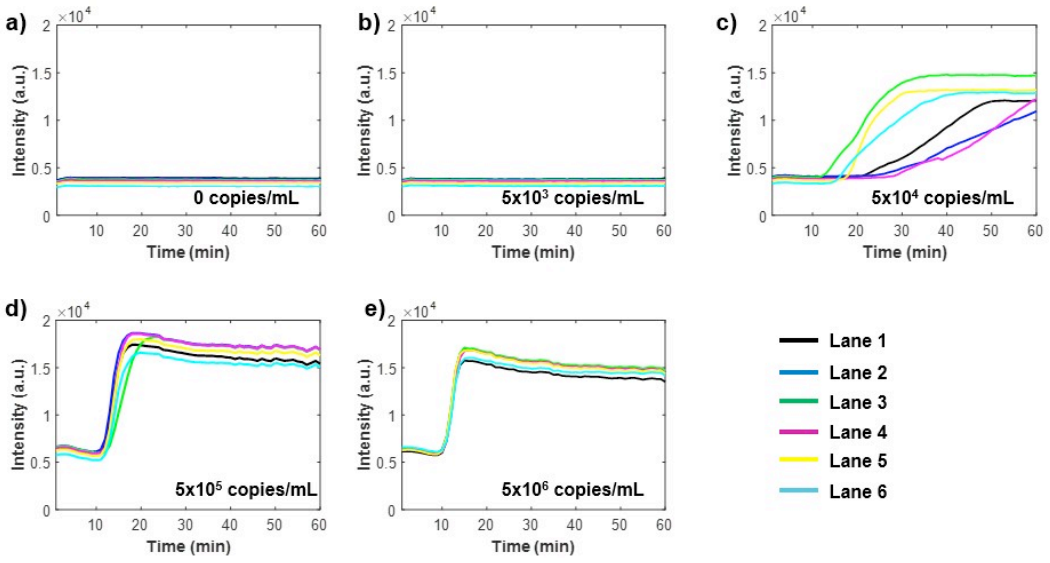

Figure 3.7: On-chip characterization of the S. Zoo assay. The negative control a) and low DNA concentration test b) show no amplification within 60 min. c) The limit of detection for the on-chip reaction is 5×10^4 copies/mL. The amplification reactions begin within 15 min for the high concentration tests at d) 5×10^5 copies/mL and e) 5×10^6 copies/mL.

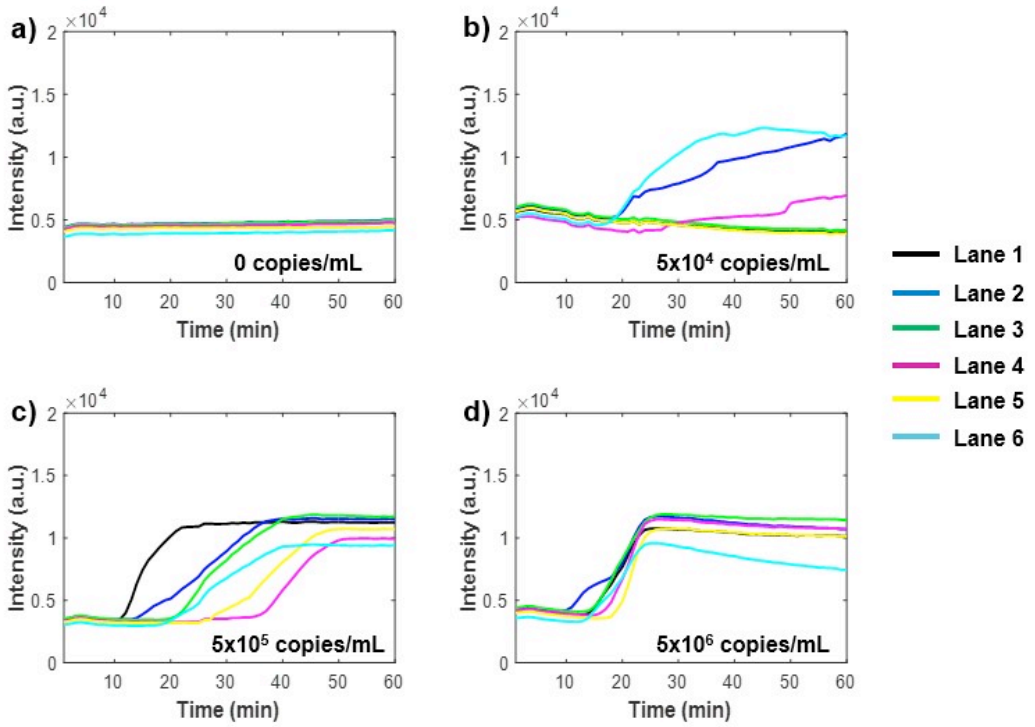

Figure 3.8: On-chip characterization of the S. Equi assay detection limit. The limit of detection for the on-chip reaction is 5×10^4 copies/mL.

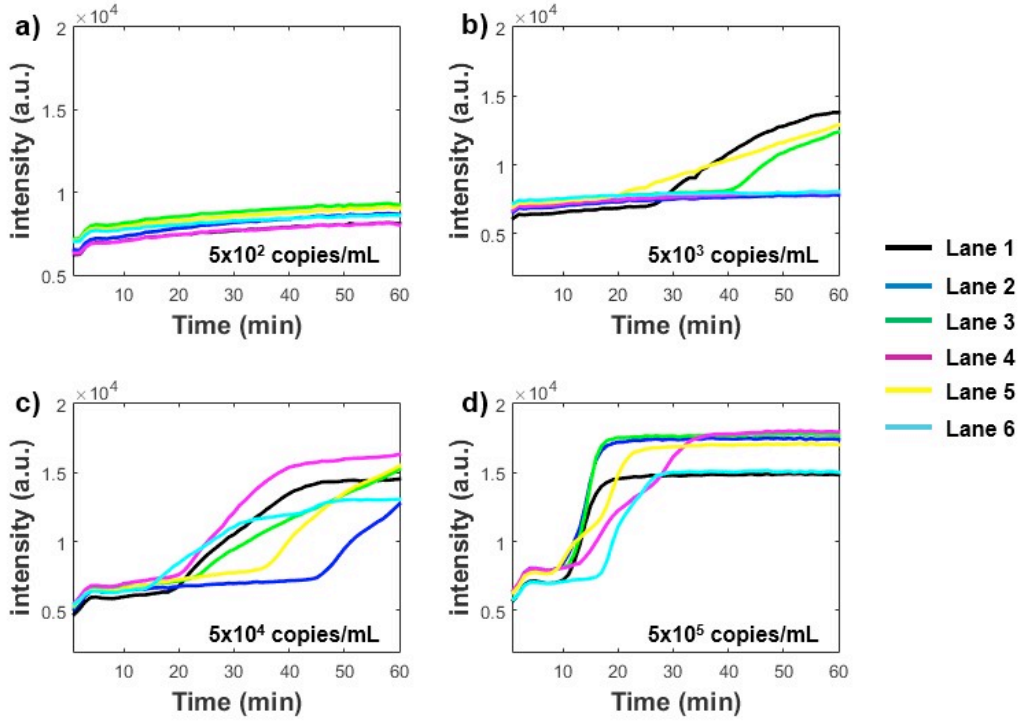

Figure 3.9: On-chip characterization of EHV-1 assay detection limit. The limit of detection for the on-chip reaction is 5×10^3 copies/mL.

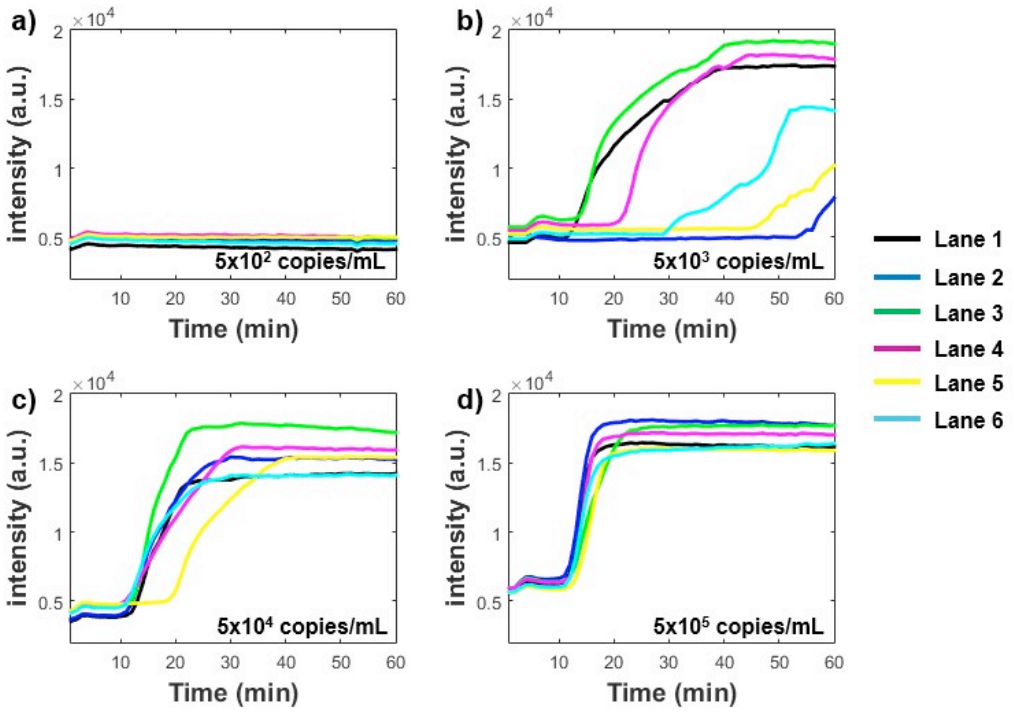

Figure 3.10: On-chip characterization of EHV-4 assay detection limit. The limit of detection for the on-chip reaction is 5×10^3 copies/mL.

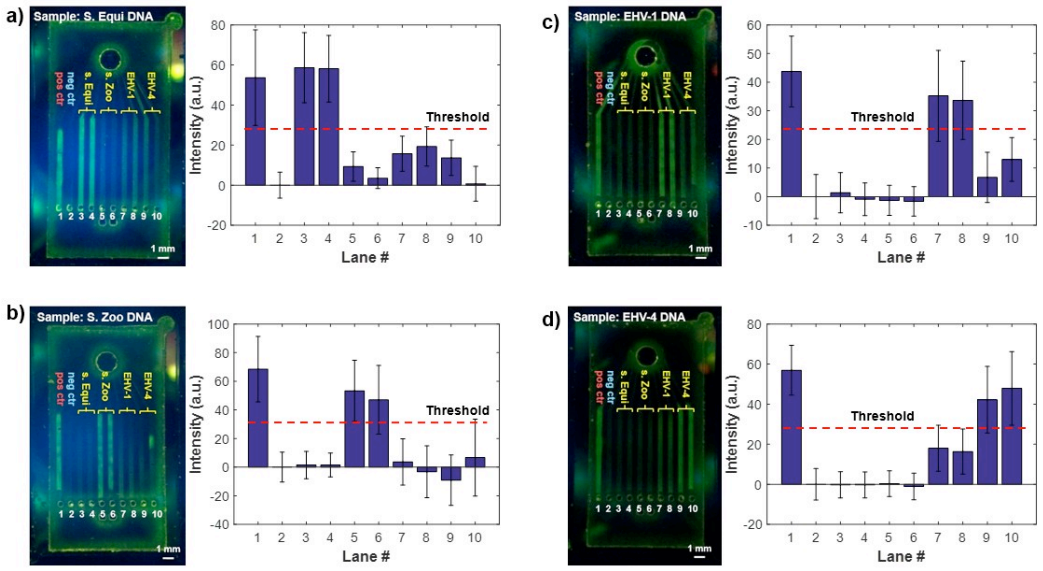

Figure 3.11: Experiments demonstrating one-at-a-time detection of target DNA sequences. Smartphone-captured images and intensities from each of the ten lanes on the fluorescence images are shown in a) for S. Equi detection, b) S. Zoo detection, c) EHV-1 detection and, d) EHV-4 detection. The LAMP reactions generate fluorescent output only in the positive control channel and the channels prepared with the specific primers. The existence of specific DNA sequence can be identified by the brightness of the lanes on the fluorescence images.

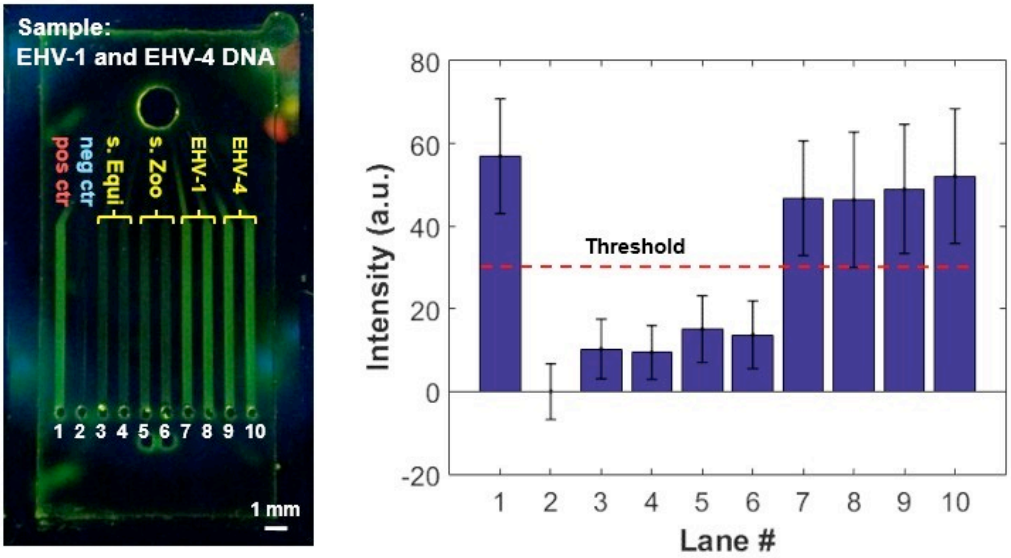

Figure 3.12: Demonstration of co-detection of multiple pathogen DNA sequences. The sample contains both the EHV-1 and EHV-4 DNA targets. Lane 1 (the positive control), lanes 7 and 8 (the lanes for EHV-1), and lanes 9 and 10 (the lanes for EHV-4) become bright after the on-chip reactions.

Table 3.1. Sequences of primers used in the LAMP assays.

Pathogens	LAMP assay primer Sequences
Streptococcus Equi	**F3**: AAA ACT AAG TGC CGG TGC2
	B3: AAA ACT AAG TGC CGG TGC2
	FIP: TAC GAC TAA CCT CAG AGT TCG CTA TCA GTA TTA GTT GCA ACA AGT G
	BIP: CGA CTC CAA GAT TAT CGC GTG ATT GAA CTT TTT GGG CTG ATG A
	Loop F: ACA GTT GTC CCT CCC AAC A
	Loop B: GCG ATA TAG CCA TAA GTG GAG ATG
	F: CGG ATA CGG TGA TGT TAA AGA
	R: TTC CTT CCT CAA AGC CAG A
Streptococcus Zooepidemicus	**F3**: AAA GAC CCT CAT GGG AAA T
	B3: CCT TAG TTG CCG CAT AGG
	FIP: CCT GAC TAA CCA AAT ATA AGC CCT TGA GCT GGA CGA TAA GAC CT
	BIP: TGT TGG ACG TAT TTT GGT TGC TCT TCT GAG CCT TCT AAA CCT G
	Loop B: GGT GTC ATT ATT AAC ATG GCC TCT
	F: CAG CAT TCC TGC TGA CAT TCG TCA GG
	R: CTG ACC AGC CTT ATT CAC AAC CAG CC
Herpesvirus 4	**F3**: CAA GAC GTA ACA ACG GGA GT
	B3: CGC AAG TAA CGG CGA TGA
	FIP: CGC TCT CCG TTT TCT TCC GAC AAG CCA CCC AGG ATT AGT CAA
	BIP: TTA CCC GGA CGG CCT TCC AAC GGG CAT GTC CTC AAC AA
	Loop F: GCC TGC TAC TCC GCA TG
	Loop B: AGC GTT GTA TAT GAT GCA TCC CCT
	F: GAC CTC TCC GTT CAC CCA AG
	R: TCC GTT TTC TTC CGA CAG GG
Herpesvirus 1	**F3**: GGC ATT TAC GTG TGG TCC TT
	B3: TCG CGG GCA TTT TTG TAC C
	FIP: GTC CAG CAA CGG TGC GTT GTG GCA CGC TCG TTA ACA GT
	BIP: CGA GCC TGA AGG GGG AAA ACT GGA GCT GTG TGG AAA GTA GC
	Loop F: AGG TTG AGA CGG TAA CGC TG
	Loop B: CAC GTG CGT CGT CGC AA
	F: GCG CCA GCT GTT TAA CCT TC
	R: CGG GCA TTT TTG TAC CAC CG

Table 3.2: Summary of the specificity of the four LAMP assays.

Template \ Primer	S.Zooep	S.Equi	EHV-1	EHV-4
S.Zooep	✓	✗	✗	✗
S.Equi	✗	✓	✗	✗
EHV-1	✗	✗	✓	✗
EHV-4	✗	✗	✗	✓

CHAPTER 4

CONCLUSON

We demonstrated mobile infectious disease detection platforms that can miniaturize the isothermal nucleic acid testing for the diagnosis of infectious diseases. A smartphone camera is used as the sensor in each platform for the measurement and analysis of the DNA amplification reactions performed on a microchip that is used to measure pathogen-specific nucleic acid sequences. The platform shown in Chapter 2 is designed for the quantitative detection of HIV in lyse whole blood, while the platform shown in Chapter 3 is able to identify the presence of multiple pathogens for equine respiratory infections.

The wide availability of smartphones has provided a novel and effective way to access patients, diagnose their health status, and manage their health information, making mobile devices a good replacement for many bulky and expensive diagnostic instruments. Because of the rapid development of mobile technologies, “mHealth” is expected to play an important role in the future of personal care and medicine. The building of a smartphone-based system for biomedical detection can help with the fast diagnosis of infectious diseases. Such capability is of great significance considering the threats brought by the outbreak of unknown infectious diseases and the re-emergence of old infectious diseases. It can also help to build an efficient and practical disease reporting system for the control and prevention of infectious diseases.

REFERENCES

[1] L. Saker, K. Lee, B. Cannito, A. Gilmore, and D. Campbell-Lendrum, "Globalization and infectious diseases: a review of the linkages," Special Programme for Research and Training in Tropical Diseases, WHO, Geneva, 2004.

[2] D. Cole, "Achievements in Public Health, 1900-1999: Control of Infectious Diseases," *Morbidity and Mortality Weekly Report,* vol. 48, no. 29, p. 621, 1999.

[3] M. L. Cohen, "Changing patterns of infectious disease," (in English), *Nature,* vol. 406, no. 6797, pp. 762-767, Aug 17 2000.

[4] D. M. Morens, G. K. Folkers, and A. S. Fauci, "The challenge of emerging and re-emerging infectious diseases," *Nature,* vol. 463, no. 7277, pp. 122-122, Jan 7 2010.

[5] "The World Health Report 2004 - Changing history," (in English), *Journal of Advanced Nursing,* vol. 48, no. 5, pp. 542-542, Dec 2004.

[6] P. S. Brachman, "Infectious diseases - past, present, and future," (in English), *International Journal of Epidemiology,* vol. 32, no. 5, pp. 684-686, Oct 2003.

[7] B. D. Gushulak and D. W. MacPherson, "Population mobility and infectious diseases: The diminishing impact of classical infectious diseases and new approaches for the 21st century," (in English), *Clinical Infectious Diseases,* vol. 31, no. 3, pp. 776-780, Sep 2000.

[8] P. Harris, "Avian Influenza: An Animal Health Issue," Animal Production and Health Division (AGA) of Food and Agriculture Organization of the United Nations, 2006, Available: http://www.fao.org/avianflu/en/issue.html.

[9] R. Alders, J. A. Awuni, B. Bagnol, P. Farrell, and N. de Haan, "Impact of Avian Influenza on Village Poultry Production Globally," (in English), *Ecohealth,* vol. 11, no. 1, pp. 63-72, Mar 2014.

[10] "The Influence of Global Environmental Change on Infectious Disease Dynamics Workshop Overview," (in English), *Influence of Global Environmental Change on Infectious Disease Dynamics: Workshop Summary,* pp. 1-109, 2014.

[11] F. Keesing *et al.*, "Impacts of biodiversity on the emergence and transmission of infectious diseases," (in English), *Nature,* vol. 468, no. 7324, pp. 647-652, Dec 2 2010.

[12] World Health Organization. (2016). *More than 2 million people coinfected with HIV and hepatitis C*. Available: http://www.who.int/hiv/mediacentre/news/hep-hiv-coinfected/en/

[13] J. K. Rockstroh and U. Spengler, "HIV and hepatitis C virus co-infection," (in English), *Lancet Infectious Diseases,* vol. 4, no. 7, pp. 437-444, Jul 2004.
[14] O. Balmer and M. Tanner, "Prevalence and implications of multiple-strain infections," (in English), *Lancet Infectious Diseases,* vol. 11, no. 11, pp. 868-878, Nov 2011.
[15] J. A. Platts-Mills, J. Liu, and E. R. Houpt, "New concepts in diagnostics for infectious diarrhea," (in English), *Mucosal Immunology,* vol. 6, no. 5, pp. 876-885, Sep 2013.
[16] G. E. Armah *et al.*, "Efficacy of pentavalent rotavirus vaccine against severe rotavirus gastroenteritis in infants in developing countries in sub-Saharan Africa: a randomised, double-blind, placebo-controlled trial," (in English), *Lancet,* vol. 376, no. 9741, pp. 606-614, Aug 21 2010.
[17] B. M. Kuehn, "IDSA: Better, Faster Diagnostics for Infectious Diseases Needed to Curb Overtreatment, Antibiotic Resistance," (in English), *Jama-Journal of the American Medical Association,* vol. 310, no. 22, pp. 2385-2386, Dec 11 2013.
[18] Y. W. Tang, G. W. Procop, and D. H. Persing, "Molecular diagnostics of infectious diseases," (in English), *Clinical Chemistry,* vol. 43, no. 11, pp. 2021-2038, Nov 1997.
[19] A. Niemz, T. M. Ferguson, and D. S. Boyle, "Point-of-care nucleic acid testing for infectious diseases," (in English), *Trends in Biotechnology,* vol. 29, no. 5, pp. 240-250, May 2011.
[20] K. Mullis, H. Erlich, N. Arnheim, G. Horn, R. Saiki, and S. Scharf, "One of the first Polymerase Chain Reaction (PCR) patents," *Google Patents,* 1987.
[21] M. Kubista *et al.*, "The real-time polymerase chain reaction," *Molecular Aspects of Medicine,* vol. 27, no. 2, pp. 95-125, 2006.
[22] T. Notomi *et al.*, "Loop-mediated isothermal amplification of DNA," (in English), *Nucleic Acids Research,* vol. 28, no. 12, Jun 15 2000.
[23] N. Tomita, Y. Mori, H. Kanda, and T. Notomi, "Loop-mediated isothermal amplification (LAMP) of gene sequences and simple visual detection of products," (in English), *Nature Protocols,* vol. 3, no. 5, pp. 877-882, 2008.
[24] M. Parida, G. Posadas, S. Inoue, F. Hasebe, and K. Morita, "Real-time reverse transcription loop-mediated isothermal amplification for rapid detection of West Nile virus," (in English), *Journal of Clinical Microbiology,* vol. 42, no. 1, pp. 257-263, Jan 2004.
[25] P. Yager *et al.*, "Microfluidic diagnostic technologies for global public health," (in English), *Nature,* vol. 442, no. 7101, pp. 412-418, Jul 27 2006.
[26] D. Mark, S. Haeberle, G. Roth, F. von Stetten, and R. Zengerle, "Microfluidic lab-on-a-chip platforms: requirements, characteristics and

applications," (in English), *Chemical Society Reviews,* vol. 39, no. 3, pp. 1153-1182, 2010.
[27] S. Park, Y. Zhang, S. Lin, T. H. Wang, and S. Yang, "Advances in microfluidic PCR for point-of-care infectious disease diagnostics," (in English), *Biotechnology Advances,* vol. 29, no. 6, pp. 830-839, Nov-Dec 2011.
[28] S. Y. Teh, R. Lin, L. H. Hung, and A. P. Lee, "Droplet microfluidics," (in English), *Lab on a Chip,* vol. 8, no. 2, pp. 198-220, 2008.
[29] S. Q. Xu *et al.*, "Generation of monodisperse particles by using microfluidics: Control over size, shape, and composition," (in English), *Angewandte Chemie-International Edition,* vol. 44, no. 5, pp. 724-728, 2005.
[30] G. M. Whitesides, "The origins and the future of microfluidics," (in English), *Nature,* vol. 442, no. 7101, pp. 368-373, Jul 27 2006.
[31] S. Law, L. Yu, A. Rosenberg, and D. Wasserman, "All-Semiconductor Plasmonic Nanoantennas for Infrared Sensing," (in English), *Nano Letters,* vol. 13, no. 9, pp. 4569-4574, Sep 2013.
[32] R. Liu *et al.*, "Mid-infrared emission from In(Ga)Sb layers on InAs(Sb)," (in English), *Optics Express,* vol. 22, no. 20, pp. 24466-24477, Oct 6 2014.
[33] A. Piruska *et al.*, "The autofluorescence of plastic materials and chips measured under laser irradiation," (in English), *Lab on a Chip,* vol. 5, no. 12, pp. 1348-1354, 2005.
[34] H. Becker and L. E. Locascio, "Polymer microfluidic devices," (in English), *Talanta,* vol. 56, no. 2, pp. 267-287, Feb 11 2002.
[35] S. R. Steinhubl, E. D. Muse, and E. J. Topol, "The emerging field of mobile health," (in English), *Science Translational Medicine,* vol. 7, no. 283, Apr 15 2015.
[36] "ICT Facts & Figures 2015 " 2016.
[37] M. A. Batista and S. M. Gaglani, "The Future of Smartphones in Health Care," *American Medical Association Journal of Ethics,* vol. 15, pp. 947-950, November 2013.
[38] "Things are looking app", *The Economist*, 2016. Available: http://www.economist.com/news/business/21694523-mobile-health-apps-are-becoming-more-capable-and-potentially-rather-useful-things-are-looking
[39] D. E. Albert, "Cardiac performance monitoring system for use with mobile communications devices," ed: Google Patents, 2014.
[40] R. G. Lee, C. C. Hsiao, C. C. Chen, and M. S. Liu, "A mobile-care system integrated with Bluetooth blood pressure and pulse monitor, and cellular phone," (in English), *IEICE Transactions on Information and Systems,* vol. E89d, no. 5, pp. 1702-1711, May 2006.
[41] L. Kwon, K. D. Long, Y. Wan, H. Yu, and B. T. Cunningham, "Medical diagnostics with mobile devices: Comparison of intrinsic and extrinsic

sensing," (in English), *Biotechnology Advances,* vol. 34, no. 3, pp. 291-304, May-Jun 2016.
[42] S. Kumar *et al.*, "Mobile Health Technology Evaluation The mHealth Evidence Workshop," (in English), *American Journal of Preventive Medicine,* vol. 45, no. 2, pp. 228-236, Aug 2013.
[43] World Health Organization. (2017). *Global Health Observatory (GHO) data*. Available: http://www.who.int/gho/hiv/en/
[44] World Health Organization, "HIV/AIDS fact sheet 2014," 2015.
[45] J. A. Aberg, J. E. Gallant, K. G. Ghanem, P. Emmanuel, B. S. Zingman, and M. A. Horberg, "Primary Care Guidelines for the Management of Persons Infected With HIV: 2013 Update by the HIV Medicine Association of the Infectious Diseases Society of America," (in English), *Clinical Infectious Diseases,* vol. 58, no. 1, pp. 1-10, Jan 1 2014.
[46] G. L. Damhorst, N. N. Watkins, and R. Bashir, "Micro- and Nanotechnology for HIV/AIDS Diagnostics in Resource-Limited Settings," (in English), *IEEE Transactions on Biomedical Engineering,* vol. 60, no. 3, pp. 715-726, Mar 2013.
[47] C. F. Rowley, "Developments in CD4 and Viral Load Monitoring in Resource-Limited Settings," (in English), *Clinical Infectious Diseases,* vol. 58, no. 3, pp. 407-412, Feb 1 2014.
[48] Uunited States Food and Drug Administration, "Complete list of donor screening assays for infectious agents and HIV diagnostic assays," 2013.
[49] X. Z. Zhang, S. B. Lowe, and J. J. Gooding, "Brief review of monitoring methods for loop-mediated isothermal amplification (LAMP)," (in English), *Biosensors & Bioelectronics,* vol. 61, pp. 491-499, Nov 15 2014.
[50] M. P. de Baar, E. C. Timmer, M. Bakker, E. de Rooij, B. van Gemen, and J. Goudsmit, "One-tube real-time isothermal amplification assay to identify and distinguish human immunodeficiency virus type 1 subtypes A, B, and C and circulating recombinant forms AE and AG," (in English), *Journal of Clinical Microbiology,* vol. 39, no. 5, pp. 1895-1902, May 2001.
[51] M. P. de Baar *et al.*, "Single rapid real-time monitored isothermal RNA amplification assay for quantification of human immunodeficiency virus type 1 isolates from groups M, N, and O," (in English), *Journal of Clinical Microbiology,* vol. 39, no. 4, pp. 1378-1384, Apr 2001.
[52] K. A. Curtis *et al.*, "Isothermal Amplification Using a Chemical Heating Device for Point-of-Care Detection of HIV-1," (in English), *Plos One,* vol. 7, no. 2, Feb 23 2012.
[53] K. A. Curtis, P. L. Niedzwiedz, A. S. Youngpairoj, D. L. Rudolph, and S. M. Owen, "Real-Time Detection of HIV-2 by Reverse Transcription-Loop-Mediated Isothermal Amplification," (in English), *Journal of Clinical Microbiology,* vol. 52, no. 7, pp. 2674-2676, Jul 2014.

[54] The World Bank, "Mobile phone access reaches three quarters of planet's population," 2012.
[55] Pharmaceutical Research and Manufacturers of America. (2013). *Infectious diseases key cause of U.S. deaths until 1920s*. Available: http://www.phrma.org/press-release/infectious-diseases-were-the-leading-cause-of-death-in-the-united-states-until-the-1920s
[56] Centers for Disease Control and Prevention. (2014). *National Notifiable Diseases Surveillance System*. Available: https://wwwn.cdc.gov/nndss/
[57] World Health Organization. (2014). *Influenza (seasonal) Fact Sheet*. Available: http://www.who.int/mediacentre/factsheets/fs211/en/
[58] N. M. Ferguson, D. A. T. Cummings, C. Fraser, J. C. Cajka, P. C. Cooley, and D. S. Burke, "Strategies for mitigating an influenza pandemic," (in English), *Nature,* vol. 442, no. 7101, pp. 448-452, Jul 27 2006.
[59] S. H. Lee, S. W. Kim, J. Y. Kang, and C. H. Ahn, "A polymer lab-on-a-chip for reverse transcription (RT)-PCR based point-of-care clinical diagnostics," (in English), *Lab on a Chip,* vol. 8, no. 12, pp. 2121-2127, 2008.
[60] J. Wang, Z. Y. Chen, P. L. A. M. Corstjens, M. G. Mauk, and H. H. Bau, "A disposable microfluidic cassette for DNA amplification and detection," (in English), *Lab on a Chip,* vol. 6, no. 1, pp. 46-53, 2006.
[61] C. S. Zhang and D. Xing, "Miniaturized PCR chips for nucleic acid amplification and analysis: latest advances and future trends," (in English), *Nucleic Acids Research,* vol. 35, no. 13, pp. 4223-4237, 2007.
[62] Z. Y. Chen *et al.*, "A microfluidic system for saliva-based detection of infectious diseases," (in English), *Oral-Based Diagnostics,* vol. 1098, pp. 429-436, 2007.
[63] D. F. Chen *et al.*, "An integrated, self-contained microfluidic cassette for isolation, amplification, and detection of nucleic acids," (in English), *Biomedical Microdevices,* vol. 12, no. 4, pp. 705-719, Aug 2010.
[64] F. Ahmad and S. A. Hashsham, "Miniaturized nucleic acid amplification systems for rapid and point-of-care diagnostics: A review," (in English), *Analytica Chimica Acta,* vol. 733, pp. 1-15, Jul 6 2012.
[65] S. L. Angione, A. Chauhan, and A. Tripathi, "Real-Time Droplet DNA Amplification with a New Tablet Platform," (in English), *Analytical Chemistry,* vol. 84, no. 6, pp. 2654-2661, Mar 20 2012.
[66] J. M. Bienvenue, L. A. Legendre, J. P. Ferrance, and J. P. Landers, "An integrated microfluidic device for DNA purification and PCR amplification of STR fragments," (in English), *Forensic Science International-Genetics,* vol. 4, no. 3, pp. 178-186, Apr 2010.
[67] M. C. Breadmore *et al.*, "Microchip-based purification of DNA from biological samples," (in English), *Analytical Chemistry,* vol. 75, no. 8, pp. 1880-1886, Apr 15 2003.

[68] N. C. Cady, S. Stelick, M. V. Kunnavakkam, and C. A. Batt, "Real-time PCR detection of Listeria monocytogenes using an integrated microfluidics platform," (in English), *Sensors and Actuators B-Chemical,* vol. 107, no. 1, pp. 332-341, May 27 2005.

[69] L. Chen, A. Manz, and P. J. R. Day, "Total nucleic acid analysis integrated on microfluidic devices," (in English), *Lab on a Chip,* vol. 7, no. 11, pp. 1413-1423, 2007.

[70] B. C. Giordano, J. Ferrance, S. Swedberg, A. F. R. Huhmer, and J. P. Landers, "Polymerase chain reaction in polymeric microchips: DNA amplification in less than 240 seconds," (in English), *Analytical Biochemistry,* vol. 291, no. 1, pp. 124-132, Apr 1 2001.

[71] J. A. Higgins *et al.*, "A handheld real time thermal cycler for bacterial pathogen detection," (in English), *Biosensors & Bioelectronics,* vol. 18, no. 9, pp. 1115-1123, Aug 15 2003.

[72] C. S. J. Hou, M. Godin, K. Payer, R. Chakrabarti, and S. R. Manalis, "Integrated microelectronic device for label-free nucleic acid amplification and detection," (in English), *Lab on a Chip,* vol. 7, no. 3, pp. 347-354, 2007.

[73] E. Kai, S. Sawata, K. Ikebukuro, T. Iida, T. Honda, and I. Karube, "Detection of PCR products in solution using surface plasmon resonance," (in English), *Analytical Chemistry,* vol. 71, no. 4, pp. 796-800, Feb 15 1999.

[74] J. Khandurina, T. E. McKnight, S. C. Jacobson, L. C. Waters, R. S. Foote, and J. M. Ramsey, "Integrated system for rapid PCR-based DNA analysis in microfluidic devices," (in English), *Analytical Chemistry,* vol. 72, no. 13, pp. 2995-3000, Jul 1 2000.

[75] M. U. Kopp, A. J. de Mello, and A. Manz, "Chemical amplification: Continuous-flow PCR on a chip," (in English), *Science,* vol. 280, no. 5366, pp. 1046-1048, May 15 1998.

[76] E. T. Lagally, I. Medintz, and R. A. Mathies, "Single-molecule DNA amplification and analysis in an integrated microfluidic device," (in English), *Analytical Chemistry,* vol. 73, no. 3, pp. 565-570, Feb 1 2001.

[77] J. H. Leamon *et al.*, "A massively parallel PicoTiterPlate (TM) based platform for discrete picoliter-scale polymerase chain reactions," (in English), *Electrophoresis,* vol. 24, no. 21, pp. 3769-3777, Nov 2003.

[78] P. G. R. Liu, J. Yang, and R. Lenigk, "Self-Contained, Fully Integrated Biochips for Sample Preparation, PCR Amplification and DNA Microarray Analysis," in *Integrated Biochips for DNA Analysis*, R. L. a. A. Lee, Ed.: Springer New York, 2007, pp. 46-67.

[79] A. L. Markey, S. Mohr, and P. J. R. Day, "High-throughput droplet PCR," (in English), *Methods,* vol. 50, no. 4, pp. 277-281, Apr 2010.

[80] S. Mohr *et al.*, "Numerical and experimental study of a droplet-based PCR chip," (in English), *Microfluidics and Nanofluidics,* vol. 3, no. 5, pp. 611-621, Oct 2007.
[81] A. F. Sauer-Budge, P. Mirer, A. Chatterjee, C. M. Klapperich, D. Chargin, and A. Sharon, "Low cost and manufacturable complete microTAS for detecting bacteria," (in English), *Lab on a Chip,* vol. 9, no. 19, pp. 2803-2810, 2009.
[82] F. Shen, W. B. Du, J. E. Kreutz, A. Fok, and R. F. Ismagilov, "Digital PCR on a SlipChip," (in English), *Lab on a Chip,* vol. 10, no. 20, pp. 2666-2672, 2010.
[83] R. Tewhey *et al.*, "Microdroplet-based PCR enrichment for large-scale targeted sequencing," (in English), *Nature Biotechnology,* vol. 27, no. 11, pp. 1025-U94, Nov 2009.
[84] F. Wang and M. A. Burns, "Performance of nanoliter-sized droplet-based microfluidic PCR," (in English), *Biomedical Microdevices,* vol. 11, no. 5, pp. 1071-1080, Oct 2009.
[85] W. Wang, Z. X. Li, R. Luo, S. H. Lu, A. D. Xu, and Y. J. Yang, "Droplet-based micro oscillating-flow PCR chip," (in English), *Journal of Micromechanics and Microengineering,* vol. 15, no. 8, pp. 1369-1377, Aug 2005.
[86] L. C. Waters, S. C. Jacobson, N. Kroutchinina, J. Khandurina, R. S. Foote, and J. M. Ramsey, "Microchip device for cell lysis, multiplex PCR amplification, and electrophoretic sizing," (in English), *Analytical Chemistry,* vol. 70, no. 1, pp. 158-162, Jan 1 1998.
[87] S. W. Yeung, T. M. H. Lee, H. Cai, and I. M. Hsing, "A DNA biochip for on-the-spot multiplexed pathogen identification," (in English), *Nucleic Acids Research,* vol. 34, no. 18, Oct 2006.
[88] C. S. Zhang, J. L. Xu, W. L. Ma, and W. L. Zheng, "PCR microfluidic devices for DNA amplification," (in English), *Biotechnology Advances,* vol. 24, no. 3, pp. 243-284, May-Jun 2006.
[89] Y. H. Zhang and P. Ozdemir, "Microfluidic DNA amplification-A review," (in English), *Analytica Chimica Acta,* vol. 638, no. 2, pp. 115-125, Apr 13 2009.
[90] N. R. Beer *et al.*, "On-chip, real-time, single-copy polymerase chain reaction in picoliter droplets," (in English), *Analytical Chemistry,* vol. 79, no. 22, pp. 8471-8475, Nov 15 2007.
[91] O. J. Dressler, R. M. Maceiczyk, S. I. Chang, and A. J. deMello, "Droplet-Based Microfluidics Enabling Impact on Drug Discovery," (in English), *Journal of Biomolecular Screening,* vol. 19, no. 4, pp. 483-496, Apr 2014.
[92] J. Liu, M. Enzelberger, and S. Quake, "A nanoliter rotary device for polymerase chain reaction," (in English), *Electrophoresis,* vol. 23, no. 10, pp. 1531-1536, May 2002.

[93] Y. Schaerli and F. Hollfelder, "The potential of microfluidic water-in-oil droplets in experimental biology," (in English), *Molecular Biosystems,* vol. 5, no. 12, pp. 1392-1404, 2009.
[94] L. G. Carrascosa, A. Calle, and L. M. Lechuga, "Label-free detection of DNA mutations by SPR: application to the early detection of inherited breast cancer," (in English), *Analytical and Bioanalytical Chemistry,* vol. 393, no. 4, pp. 1173-1182, Feb 2009.
[95] T. Endo, K. Kerman, N. Nagatani, Y. Takamura, and E. Tamiya, "Label-free detection of peptide nucleic acid-DNA hybridization using localized surface plasmon resonance based optical biosensor," (in English), *Analytical Chemistry,* vol. 77, no. 21, pp. 6976-6984, Nov 1 2005.
[96] H. X. Li and L. J. Rothberg, "Label-free colorimetric detection of specific sequences in genomic DNA amplified by the polymerase chain reaction," (in English), *Journal of the American Chemical Society,* vol. 126, no. 35, pp. 10958-10961, Sep 8 2004.
[97] A. T. Woolley, D. Hadley, P. Landre, A. J. deMello, R. A. Mathies, and M. A. Northrup, "Functional integration of PCR amplification and capillary electrophoresis in a microfabricated DNA analysis device," (in English), *Analytical Chemistry,* vol. 68, no. 23, pp. 4081-4086, Dec 1 1996.
[98] D. C. Zhang *et al.*, "Label-free and high-sensitive detection of Salmonella using a surface plasmon resonance DNA-based biosensor," (in English), *Journal of Biotechnology,* vol. 160, no. 3-4, pp. 123-128, Aug 31 2012.
[99] J. Compton, "Nucleic-Acid Sequence-Based Amplification," (in English), *Nature,* vol. 350, no. 6313, pp. 91-92, Mar 7 1991.
[100] G. T. Walker, M. S. Fraiser, J. L. Schram, M. C. Little, J. G. Nadeau, and D. P. Malinowski, "Strand Displacement Amplification - an Isothermal, Invitro DNA Amplification Technique," (in English), *Nucleic Acids Research,* vol. 20, no. 7, pp. 1691-1696, Apr 11 1992.
[101] O. Piepenburg, C. H. Williams, D. L. Stemple, and N. A. Armes, "DNA detection using recombination proteins," (in English), *Plos Biology,* vol. 4, no. 7, pp. 1115-1121, Jul 2006.
[102] R. D. Stedtfeld *et al.*, "Gene-Z: a device for point of care genetic testing using a smartphone," (in English), *Lab on a Chip,* vol. 12, no. 8, pp. 1454-1462, 2012.
[103] C. Duarte, E. Salm, B. Dorvel, B. Reddy, and R. Bashir, "On-chip parallel detection of foodborne pathogens using loop-mediated isothermal amplification," (in English), *Biomedical Microdevices,* vol. 15, no. 5, pp. 821-830, Oct 2013.
[104] P. Craw and W. Balachandran, "Isothermal nucleic acid amplification technologies for point-of-care diagnostics: a critical review," (in English), *Lab on a Chip,* vol. 12, no. 14, pp. 2469-2486, 2012.

[105] M. Parida, S. Sannarangaiah, P. K. Dash, P. V. L. Rao, and K. Morita, "Loop mediated isothermal amplification (LAMP): a new generation of innovative gene amplification technique; perspectives in clinical diagnosis of infectious diseases," (in English), *Reviews in Medical Virology,* vol. 18, no. 6, pp. 407-421, Nov-Dec 2008.

[106] W. L. Chen *et al.*, "Planar Photonic Crystal Biosensor for Quantitative Label-Free Cell Attachment Microscopy," (in English), *Advanced Optical Materials,* vol. 3, no. 11, pp. 1623-1632, Nov 2015.

[107] W. L. Chen *et al.*, "Photonic crystal enhanced microscopy for imaging of live cell adhesion," (in English), *Analyst,* vol. 138, no. 20, pp. 5886-5894, 2013.

[108] W. L. Chen *et al.*, "Enhanced live cell imaging via photonic crystal enhanced fluorescence microscopy," (in English), *Analyst,* vol. 139, no. 22, pp. 5954-5963, Nov 21 2014.

[109] R. D. Peterson, W. L. Chen, B. T. Cunningham, and J. E. Andrade, "Enhanced sandwich immunoassay using antibody-functionalized magnetic iron-oxide nanoparticles for extraction and detection of soluble transferrin receptor on a photonic crystal biosensor," (in English), *Biosensors & Bioelectronics,* vol. 74, pp. 815-822, Dec 15 2015.

[110] Y. Zhuo *et al.*, "Single nanoparticle detection using photonic crystal enhanced microscopy," (in English), *Analyst,* vol. 139, no. 5, pp. 1007-1015, 2014.

[111] Frost & Sullivan, "Global Analysis of the Smartphones Market: Who's Winning the Necessary Regional Battles," 2013.

[112] G. Comtois, J. I. Salisbury, and Y. Sun, "A Smartphone-Based Platform for Analyzing Physiological Audio Signals," (in English), *2012 38th Annual Northeast Bioengineering Conference (Nebec),* pp. 69-70, 2012.

[113] C. C. Huang, P. Y. Lee, P. Y. Chen, and T. Y. Liu, "Design and Implementation of a Smartphone-Based Portable Ultrasound Pulsed-Wave Doppler Device for Blood Flow Measurement," (in English), *IEEE Transactions on Ultrasonics Ferroelectrics and Frequency Control,* vol. 59, no. 1, pp. 182-188, Jan 2012.

[114] D. N. Breslauer, R. N. Maamari, N. A. Switz, W. A. Lam, and D. A. Fletcher, "Mobile Phone Based Clinical Microscopy for Global Health Applications," (in English), *Plos One,* vol. 4, no. 7, Jul 22 2009.

[115] Q. S. Wei *et al.*, "Fluorescent Imaging of Single Nanoparticles and Viruses on a Smart Phone," (in English), *ACS Nano,* vol. 7, no. 10, pp. 9147-9155, Oct 2013.

[116] G. L. Damhorst, C. Duarte-Guevara, W. Chen, T. Ghonge, B. T. Cunningham, and R. Bashir, "Smartphone-Imaged HIV-1 Reverse-Transcription Loop-Mediated Isothermal Amplification (RT-LAMP) on a Chip from Whole Blood," *Engineering,* vol. 1, no. 3, pp. 324 -335, 2015.

[117] D. Gallegos *et al.*, "Label-free biodetection using a smartphone," (in English), *Lab on a Chip,* vol. 13, no. 11, pp. 2124-2132, 2013.
[118] J. Jiang *et al.*, "Smartphone based portable bacteria pre-concentrating microfluidic sensor and impedance sensing system," (in English), *Sensors and Actuators B-Chemical,* vol. 193, pp. 653-659, Mar 2014.
[119] H. J. Yu, Y. F. Tan, and B. T. Cunningham, "Smartphone Fluorescence Spectroscopy," (in English), *Analytical Chemistry,* vol. 86, no. 17, pp. 8805-8813, Sep 2 2014.
[120] K. D. Long, H. Yu, and B. T. Cunningham, "Smartphone instrument for portable enzyme-linked immunosorbent assays," (in English), *Biomedical Optics Express,* vol. 5, no. 11, pp. 3792-3806, Nov 1 2014.
[121] D. Erickson *et al.*, "Smartphone technology can be transformative to the deployment of lab-on-chip diagnostics," (in English), *Lab on a Chip,* vol. 14, no. 17, pp. 3159-3164, 2014.
[122] C. F. Fronczek, T. S. Park, D. K. Harshman, A. M. Nicolini, and J. Y. Yoon, "Paper microfluidic extraction and direct smartphone-based identification of pathogenic nucleic acids from field and clinical samples," (in English), *RSC Advances,* vol. 4, no. 22, pp. 11103-11110, 2014.
[123] S. C. B. Gopinath, T. H. Tang, Y. Chen, M. Citartan, and T. Lakshmipriya, "Bacterial detection: From microscope to smartphone," (in English), *Biosensors & Bioelectronics,* vol. 60, pp. 332-342, Oct 15 2014.
[124] L. Jiang, M. Mancuso, Z. D. Lu, G. Akar, E. Cesarman, and D. Erickson, "Solar thermal polymerase chain reaction for smartphone-assisted molecular diagnostics," (in English), *Scientific Reports,* vol. 4, Feb 20 2014.
[125] J.-D. Kim, Y.-S. Kim, H.-J. Song, and C. Y. Park, "Development of PCR Control Software for Smartphone Using both Wired and Wireless Communications," *International Journal of Multimedia and Ubiquitous Engineering,* vol. 8, pp. 223-230, 2013.
[126] X. Y. Liu, T. Y. Lin, and P. B. Lillehoj, "Smartphones for Cell and Biomolecular Detection," (in English), *Annals of Biomedical Engineering,* vol. 42, no. 11, pp. 2205-2217, Nov 2014.
[127] P. Duarte-Guevara, C. Duarte-Guevara, A. Ornob, and R. Bashir, "On-chip PMA labeling of foodborne pathogenic bacteria for viable qPCR and qLAMP detection," (in English), *Microfluidics and Nanofluidics,* vol. 20, no. 8, Aug 2016.
[128] M. Nemoto, K. Tsujimura, T. Yamanaka, T. Kondo, and T. Matsumura, "Loop-mediated isothermal amplification assays for detection of Equid herpesvirus 1 and 4 and differentiating a gene-deleted candidate vaccine strain from wild-type Equid herpesvirus 1 strains," (in English), *Journal of Veterinary Diagnostic Investigation,* vol. 22, no. 1, pp. 30-36, Jan 2010.

[129] J. Canny, "A Computational Approach to Edge-Detection," (in English), *IEEE Transactions on Pattern Analysis and Machine Intelligence,* vol. 8, no. 6, pp. 679-698, Nov 1986.
[130] C. Carignan, R. K. Shosted, M. J. Fu, Z. P. Liang, and B. P. Sutton, "A real-time MRI investigation of the role of lingual and pharyngeal articulation in the production of the nasal vowel system of French," (in English), *Journal of Phonetics,* vol. 50, pp. 34-51, May 2015.
[131] M. J. Fu, M. S. Barlaz, R. K. Shosted, Z. P. Liang, and B. P. Sutton, "High-Resolution Dynamic Speech Imaging with Deformation Estimation," (in English), *2015 37th Annual International Conference of the IEEE Engineering in Medicine and Biology Society (Embc),* pp. 1568-1571, 2015.
[132] M. J. Fu, J. Woo, Z. P. Liang, and B. P. Sutton, "Spatiotemporal-atlas-based Dynamic Speech Imaging," (in English), *Medical Imaging 2016-Biomedical Applications in Molecular, Structural, and Functional Imaging,* vol. 9788, 2016.
[133] M. J. Fu *et al.*, "High-Resolution Dynamic Speech Imaging with Joint Low-Rank and Sparsity Constraints," (in English), *Magnetic Resonance in Medicine,* vol. 73, no. 5, pp. 1820-1832, May 2015.
[134] M. J. Fu, J. J. Zhuang, F. Z. Hou, X. B. Ning, Q. B. Zhan, and Y. Shao, "Extracting human gait series based on the wavelet transform," (in Chinese), *Acta Physica Sinica,* vol. 59, no. 6, pp. 4343-4350, Jun 2010.
[135] J. D. Gai *et al.*, "More IMPATIENT: A gridding-accelerated Toeplitz-based strategy for non-Cartesian high-resolution 3D MRI on GPUs," (in English), *Journal of Parallel and Distributed Computing,* vol. 73, no. 5, pp. 686-697, May 2013.
[136] F. Z. Hou, X. B. Ning, J. J. Zhuang, X. L. Huang, M. J. Fu, and C. H. Bian, "High-dimensional time irreversibility analysis of human interbeat intervals," (in English), *Medical Engineering & Physics,* vol. 33, no. 5, pp. 633-637, Jun 2011.
[137] X. L. Wu *et al.*, "Impatient Mri: Illinois Massively Parallel Acceleration Toolkit for Image Reconstruction with Enhanced Throughput in Mri," (in English), *2011 8th IEEE International Symposium on Biomedical Imaging: From Nano to Macro,* pp. 69-72, 2011.
[138] B. Rush and T. Mair, *Equine Respiratory Diseases: Blackwell Publishing*. Blackwell Publishing, 2004.
[139] L. Viel and D. Jean, "Inflammatory Airway Disease " in *Blackwell's Five-Minute Veterinary Consult: Equine*, J.-P. Lavoie and K. W. Hinchcliff, Eds.: Wiley-Blackwell Publishing, 2008.
[140] L. Couetil and J. Hawkins, *Respiratory Diseases of the Horse: A Problem-Oriented Approach to Diagnosis and Management*. Mason Publishing, 2013.

[141] J. M. Love, R. Marquis-Nicholson, R. C. Love, and D. R. Love, "Portable Battery-Operated Rapid PCR Amplification of the CAG Repeat Region of the Huntington Disease Locus " *Research Journal of Biology,* vol. 02, no. 06, pp. 191-196 2012.
[142] M. A. Poritz *et al.*, "FilmArray, an Automated Nested Multiplex PCR System for Multi-Pathogen Detection: Development and Application to Respiratory Tract Infection," (in English), *Plos One,* vol. 6, no. 10, Oct 19 2011.
[143] T. Abe *et al.*, "Point-of-care testing system enabling 30 min detection of influenza genes," (in English), *Lab on a Chip,* vol. 11, no. 6, pp. 1166-1167, 2011.
[144] C. Toumazou *et al.*, "Simultaneous DNA amplification and detection using a pH-sensing semiconductor system," (in English), *Nature Methods,* vol. 10, no. 7, pp. 641-+, Jul 2013.
[145] A. S. Patterson, K. Hsieh, H. T. Soh, and K. W. Plaxco, "Electrochemical real-time nucleic acid amplification: towards point-of-care quantification of pathogens," (in English), *Trends in Biotechnology,* vol. 31, no. 12, pp. 704-712, Dec 2013.
[146] F. L. Kiechle and C. A. Holland, "Point-of-Care Testing and Molecular Diagnostics: Miniaturization Required," (in English), *Clinics in Laboratory Medicine,* vol. 29, no. 3, pp. 555-+, Sep 2009.
[147] Y. Kinoshita, H. Niwa, and Y. Katayama, "Development of a Loop-Mediated Isothermal Amplification Method for Detecting Streptococcus equi subsp zooepidemicus and Analysis of Its Use with Three Simple Methods of Extracting DNA from Equine Respiratory Tract Specimens," (in English), *Journal of Veterinary Medical Science,* vol. 76, no. 9, pp. 1271-1275, Sep 2014.
[148] C. J. Easley *et al.*, "A fully integrated microfluidic genetic analysis system with sample-in-answer-out capability," (in English), *Proceedings of the National Academy of Sciences of the United States of America,* vol. 103, no. 51, pp. 19272-19277, Dec 19 2006.
[149] K. A. Hagan, C. R. Reedy, M. L. Uchimoto, D. Basu, D. A. Engel, and J. P. Landers, "An integrated, valveless system for microfluidic purification and reverse transcription-PCR amplification of RNA for detection of infectious agents," (in English), *Lab on a Chip,* vol. 11, no. 5, pp. 957-961, 2011.
[150] L. A. Legendre, J. M. Bienvenue, M. G. Roper, J. P. Ferrance, and J. P. Landers, "A simple, valveless microfluidic sample preparation device for extraction and amplification of DNA from nanoliter-volume samples," (in English), *Analytical Chemistry,* vol. 78, no. 5, pp. 1444-1451, Mar 1 2006.
[151] U. B. R. Balasuriya, B. M. Crossley, and P. J. Timoney, "A review of traditional and contemporary assays for direct and indirect detection of Equid herpesvirus 1 in clinical samples," (in English), *Journal of*

Veterinary Diagnostic Investigation, vol. 27, no. 6, pp. 673-687, Nov 2015.